

AD-A051 394

ROCKWELL INTERNATIONAL CEDAR RAPIDS IOWA COLLINS RA--ETC F/G 9/5
TRANSCEIVER MULTICOUPLERS.(U)
SEP 76 H L LANDT

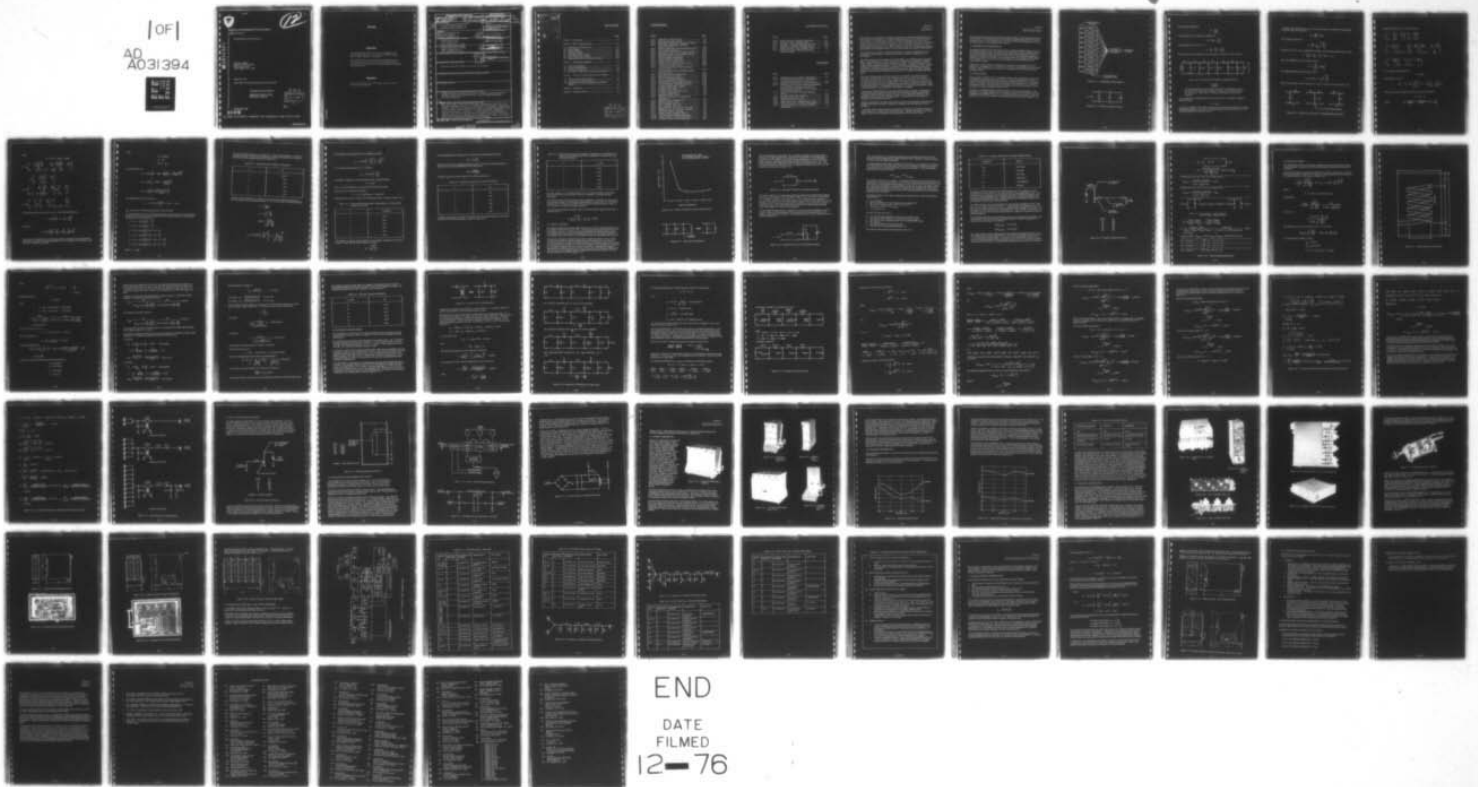
UNCLASSIFIED

ECOM-75-0113-F

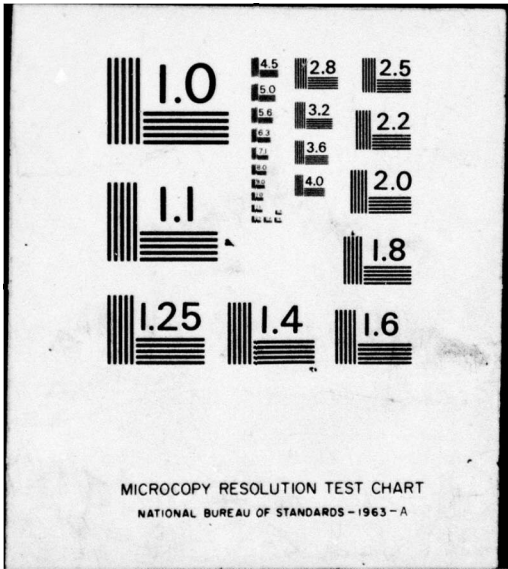
DAAB07-75-C-0113
NL

| of |

AD
A031394



END
DATE
FILMED
12-76





12 78

Research and Development Technical Report
ECOM- 75-0113-F

TRANSCEIVER MULTICOUPLER

AD A 031394

Harvey L. Landt
COLLINS RADIO GROUP
5225 C Avenue N.E.
Cedar Rapids, Iowa 52406

September 1976

Final Report for Period February 1975 to July 1976

DISTRIBUTION STATEMENT

Approved for public release;
distribution unlimited.

DDC
RECEIVED
NOV 1 1976
D

Q

PREPARED FOR:

ECOM

US ARMY ELECTRONICS COMMAND FORT MONMOUTH, NEW JERSEY 07703

NOTICES

Disclaimers

The findings in this report are not to be construed as an official Department of the Army position, unless so designated by other authorized documents.

The citation of trade names and names of manufacturers in this report is not to be construed as official Government indorsement or approval of commercial products or services referenced herein.

Disposition

Destroy this report when it is no longer needed. Do not return it to the originator.

REPORT DOCUMENTATION PAGE		READ INSTRUCTIONS BEFORE COMPLETING FORM	
1. REPORT NUMBER 18 ECOM-75-0113-F	2. GOVT ACCESSION NO. 9 Final rept. 15 Feb - 15 Jul 76	3. RECIPIENT'S CATALOG NUMBER	
4. TITLE (and Subtitle) 6 Transceiver Multicoupler		5. TYPE OF REPORT & PERIOD COVERED Final Feb 15, 75 to Jul 15, 76	
7. AUTHOR(s) 10 HARVEY L. LANDT		6. PERFORMING ORG. REPORT NUMBER 523-0767328-00121L	
9. PERFORMING ORGANIZATION NAME AND ADDRESS Collins Radio Group 5225 C Avenue N.E. Cedar Rapids, Iowa 52406		8. CONTRACT OR GRANT NUMBER(s) 15 DAAB07-75-C-0113 <i>new</i>	
11. CONTROLLING OFFICE NAME AND ADDRESS US Army Electronics Command ATTN: DRSEL-NL-RN-3 Fort Monmouth, NJ 07703		10. PROGRAM ELEMENT, PROJECT, TASK AREA & WORK UNIT NUMBERS 1X7637 07 D437 0709	
14. MONITORING AGENCY NAME & ADDRESS (if different from Controlling Office)		12. REPORT DATE 11 September 1976	
		13. NUMBER OF PAGES 70	
	12 51 P.	15. SECURITY CLASS. (of this report) Unclassified	
16. DISTRIBUTION STATEMENT (of this Report) Approved for Public Release, distribution unlimited		15a. DECLASSIFICATION/DOWNGRADING SCHEDULE	
17. DISTRIBUTION STATEMENT (of the abstract entered in Block 20, if different from Report)			
18. SUPPLEMENTARY NOTES			
19. KEY WORDS (Continue on reverse side if necessary and identify by block number) Antenna Couplers, Antenna Multicouplers, Broadband Combining Networks, Broadband Coupling, Coupling Circuits, Filters, Matching Networks, RF Tuning Capacitors			
20. ABSTRACT (Continue on reverse side if necessary and identify by block number) This final report covers the development, construction, and test of the advanced development models of the transceiver multicoupler. Deliverable hardware consists of a 2-channel multicoupler, 5-channel multicoupler, and a spare filter. The theoretical basis and experimental principles of the design are discussed in section 2. A description of the deliverable hardware, test results, and physical configuration are given in section 3. Section 4 discusses an alternate design approach employing a 2-pole band-pass filter in place of the present 3-pole design.			

408904

4/B

ACCESSION for

NTIS Write Section

DDC Buff Section

UNANNOUNCED

JUSTIFICATION.....

BY.....

DISTRIBUTION/AVAILABILITY CODES

ORIG. AVAIL. and/or SPECIAL

A

Table of Contents

	Page
Section 1 Introduction.....	1-1
Section 2 Basic Design Concepts	2-1
2.1 Preliminary Considerations	2-1
2.2 Filter Design.....	2-1
2.3 Output Coupling.....	2-11
2.4 Resonator Design.....	2-18
2.5 Matching Network Design.....	2-23
2.6 Input and Internal Couplings	2-36
2.7 Tuning Method and Discriminator Design.....	2-37
Section 3 Deliverable Equipment.....	3-1
3.1 General Description.....	3-1
3.2 Measured Performance	3-3
3.3 Physical Configuration	3-5
3.4 Schematics, Parts Lists, and Tuning Procedure.....	3-11
Section 4 Alternate Design Approach (2-Pole Filter).....	4-1
4.1 General Design Considerations	4-1
4.2 Advantages and Disadvantages	4-4
4.3 Specification Changes to Incorporate Alternate Design.....	4-4
Section 5 Conclusion	5-1
Section 6 Literature Cited.....	6-1

D D C
 RECEIVED
 NOV 1 1976
 RECEIVED
 D

List of Illustrations

Figure		Page
2.1-1	Multicoupler, Block Diagram	2-2
2.2-1	Resonator Equivalent Circuit.....	2-2
2.2-2	Filter With n Resonators, Equivalent Circuit.....	2-3
2.2-3	Filter With n Resonators, Resultant Equivalent Circuit	2-4
2.2-4	Number of Resonators Versus Insertion Loss.....	2-12
2.3-1	Total Junction Impedance.....	2-12
2.3-2	Equivalent Circuit of an Off-Channel Branch	2-13
2.3-3	Equivalent Circuit of an On-Channel Branch	2-13
2.3-4	Measured Output Terminal Q.....	2-16
2.3-5	Output Coupling Computations.....	2-17
2.4-1	Helical Resonator Dimensions	2-19
2.5-1	Norton's First Transformation	2-24
2.5-2	Reduction of Transformer to Final Form.....	2-25
2.5-3	Transformer Element Values	2-27
2.5-4	5-Channel Multicoupler Matching Network Element Values.....	2-32
2.5-5	10-Channel Multicoupler Matching Network Element Values.....	2-34
2.5-6	Final Multicoupler Configurations	2-35
2.6-1	Measured Input Terminal Q.....	2-36
2.6-2	Measured Coupling Coefficient.....	2-37
2.7-1	Filter, Simplified Block Diagram	2-38
2.7-2	Simplified Directional Coupler Schematic	2-38
2.7-3	90° Discriminator, Simplified Schematic.....	2-39
3.1-1	5-Channel Multicoupler (156W-2)	3-1
3.1-2	2-Channel Multicoupler (156W-1)	3-2
3.1-3	Bandpass Filter (835P-1).....	3-2
3.1-4	5-Channel Multicoupler (Rear View).....	3-2
3.1-5	2-Channel Mounting Base.....	3-2
3.2-1	Measured Insertion Loss	3-3
3.2-2	Measured Transceiver to Antenna Port Attenuation	3-4
3.3-1	Bandpass Filter, Exploded View.....	3-6
3.3-2	Helical Resonator Detail.....	3-6
3.3-3	Drive Assembly, Rear View	3-6
3.3-4	Drive Assembly, Side View	3-6
3.3-5	Filter Side View, Access Cover Removed	3-7
3.3-6	Bandpass Filter, RF Connector Locations.....	3-7
3.3-7	Directional Coupler Assembly.....	3-8
3.3-8	Outline Drawing, Bandpass Filters	3-9
3.3-9	2-Channel Network and Mounting Base	3-9
3.3-10	Outline Drawing, 2-Channel Multicoupler.....	3-10
3.3-11	5-Channel Network and Mounting Base	3-10

List of Illustrations (Cont)

Figure		Page
3.3-12	Outline Drawing, 5-Channel Multicoupler.....	3-11
3.4-1	Schematic, 835P-1 Bandpass Filter	3-12
3.4-2	Schematic, 2-Channel Combining Network.....	3-14
3.4-3	Schematic, 5-Channel Combining Network.....	3-15
4.1-1	Outline Drawing, 2-Pole Bandpass Filter.....	4-3
4.1-2	Outline Drawing, 2-Channel Multicoupler (Alternate Design)	4-3

List of Tables

Table		Page
2.2-1	Terminal Q Versus Number of Resonators.....	2-8
2.2-2	S-Dimension Versus Number of Resonators for a Total Filter Volume of 54.675 In ³	2-9
2.2-3	Resonator Unloaded Q for a 54.675-In ³ Filter.....	2-10
2.2-4	Insertion Loss Versus the Number of Resonators for a Minimum Loss Filter of 54.675 In ³ , Having 40 dB of Attenuation 5 Percent From the Operating Frequency.....	2-11
2.3-1	Optimum Parameters for Output Coupling Circuit	2-15
2.4-1	Resonator Measured Unloaded Q	2-23
3.2-1	Measured Performance Data.....	3-5
3.4-1	VHF Filter 835P-1, Parts List.....	3-13
3.4-2	156W-1 Parts List, 2-Channel Multicoupler.....	3-15
3.4-3	156W-2 Parts List, 5-Channel Multicoupler.....	3-16
3.4-4	Tuning Procedure for the 156W-1/156W-2 Multicoupler.....	3-17

Section 1

Introduction

This report covers the design, fabrication, and test of a multicoupler that permits up to 10 transceivers to operate from a single broadband antenna over the frequency range of 30 to 80 MHz. The multicouplers consist of identical, manually tuned, 3-pole filter modules mounted on a common mounting base. The mounting base contains a combining/matching network that allows the rf output terminals of the filter modules to be connected together and operated on a common antenna. Electronics Command Development Specification DS-AF-0169A(A) dated 21 June 1974 describes the required multicouplers.

On this particular contract a 2-channel multicoupler, 5-channel multicoupler, and a spare filter were developed. The design, however, includes the capability of up to 10 channels.

The filter design, for each channel of the multicoupler, is a minimum loss 3-resonator filter. Each resonator of the filter consists of a capacitively tuned helical resonator. Fixed coupling structures are used throughout the filter. This provides a practical, simple, easily reproducible design. The internal aperture couplings provide a constant coefficient of coupling as the filter is tuned over the operating frequency range, thus providing a constant percentage bandwidth characteristic. Input and output couplings provide a nearly constant terminal Q as required for a constant percentage bandwidth filter.

The input coupling employs a fixed series inductor tapped into the input resonator. This form of coupling provides good coupling characteristics along with minimum resonator frequency shift. The output coupling must be such that up to 10 filters may be connected together to form a multicoupler. This output coupling in conjunction with the interconnecting lines and a broadband matching network provides the desired multicoupler performance. The broadband matching network requires no adjustment, tuning, or band switching, as the frequency of the channels is changed.

Overall measured performance of the deliverable hardware is good. No tuning interaction between the channels has been observed for frequency spacings greater than 5 percent. Details of the test circuits, results, and test equipment used, have been presented in the contractor's evaluation report. A summary of the measured performance is presented in this report.

Detailed schematics of the filter and matching networks are presented. Constructional details of the helical resonators, apertures, couplings, and matching networks are included.

An alternate filter design employing 2 resonators instead of 3 is presented. This approach allows for a simpler more economical filter. Design trade-offs are discussed, together with a list of advantages and disadvantages of the alternate design.

In this section the basic ideas and design concepts leading to the deliverable equipment are discussed. The theoretical basis is formulated, together with measured data supporting the theory. The information and concepts have been formulated over a period of several years, and are unified in this section.

2.1 PRELIMINARY CONSIDERATIONS

It is desired to operate up to 10 transceivers on a single broadband antenna in the 30- to 80-MHz frequency range. This has been accomplished by using a selective filter in each communication channel and connecting the filter outputs in parallel through an appropriate combining/matching network. Since various multicoupler configurations (number of channels) are desired, it is advantageous to use an identical filter design in all configurations. Also the matching/combining networks should have some commonality in design.

Figure 2.1-1 depicts the basic configuration employed. The matching network is installed in a mounting base. The filters are removable, individually, from the mounting base. Push-on connectors provide the rf connection between the filters and the matching network.

2.2 FILTER DESIGN

The first area of concern is the overall filter design. The specification requires the multicouplers to provide 40 dB of attenuation at a frequency spacing of 5 percent. It is also required that the filters have the lowest possible insertion loss in a minimum volume. To achieve the best possible selectivity versus insertion loss a minimum-loss design is used. The approach to determining the performance parameters and arriving at an optimum design is detailed below.

The filter is composed of parallel-tuned circuits or resonators of quantity n . The resonators are coupled together by $n-1$ coupling elements. It has been shown that the minimum-loss condition occurs when all elements of the filter are equal.¹ Thus, the equivalent circuit for all resonators comprising the filter is as shown in figure 2.2-1.

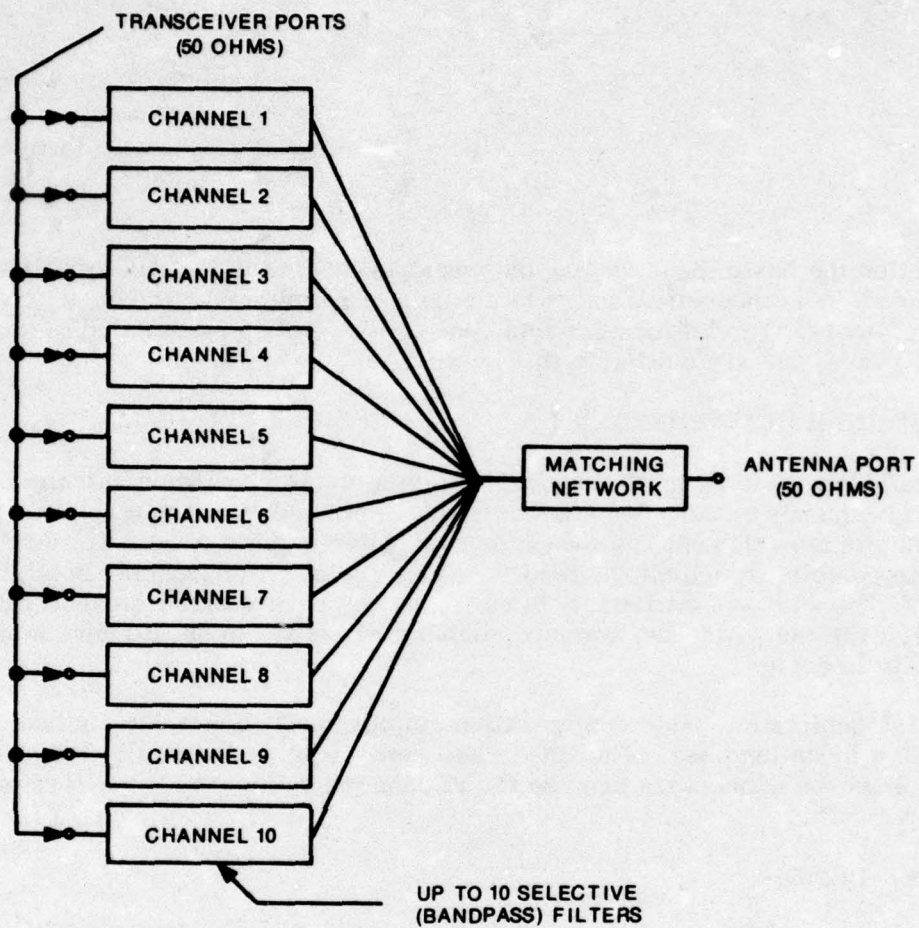


Figure 2.1-1. Multicoupler, Block Diagram.

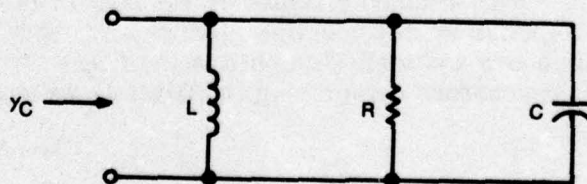


Figure 2.2-1. Resonator Equivalent Circuit.

The resonant frequency is:

$$\omega_0 = \frac{1}{\sqrt{LC}}$$

The unloaded Q of the resonator is defined as:

$$Q_u = R\omega_0 C = \frac{R}{\omega_0 L}$$

The admittance of the circuit is:

$$Y_c = \frac{1}{R} + j\left(\omega C - \frac{1}{\omega L}\right)$$

The resonators are combined as shown in figure 2.2-2 to form a filter network.

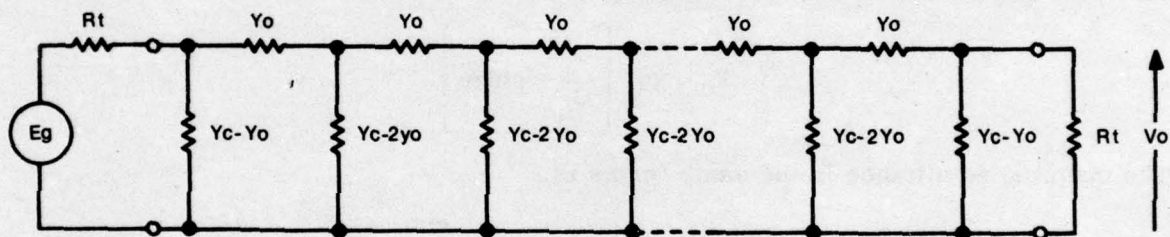


Figure 2.2-2. Filter With n Resonators, Equivalent Circuit.

Note

The above network has been synchronously tuned as indicated. All but the two end shunt elements are equal to $Y_c - 2Y_o$, and all series elements are equal to Y_o . There are $n-1$ series elements and $n-2$ equal shunt elements.

The resonators are coupled together by an admittance Y_o . Capacitive coupling is assumed, that is:

$$Y_o = j\omega C_o$$

The type of coupling element used in the analysis is immaterial because of the narrow bandwidth of the filter. Any form of coupling would give the same result for a filter having a bandwidth of 10 percent or less.

A terminal Q is defined, that is, the Q of the end resonators loaded by the terminating resistance only, and is given by:

$$Q_t = \frac{R_t}{\omega_0 L} = R_t \omega_0 C$$

The coupling coefficient is:

$$k = \frac{C_o}{C} = \frac{1}{Q_t} \sqrt{1 + \frac{Q_t}{Q_u}}$$

Because of the very narrow bandwidth of the filter, the following approximation is used:

$$U = \frac{\omega - \omega_0}{\omega} \approx \frac{\omega}{\omega_0} - \frac{\omega_0}{\omega} \quad \text{where: } U \ll 1$$

Thus, the admittance of the resonator becomes:

$$Y_c = G_t \left[\frac{Q_t}{Q_u} + j2Q_t u \right]$$

The coupling admittance in the same terms is:

$$Y_o = jG_t k Q_t = jG_t \sqrt{1 + \frac{Q_t}{Q_u}}$$

The two port network shown in figure 2.2-2 may be redrawn as shown in figure 2.2-3.

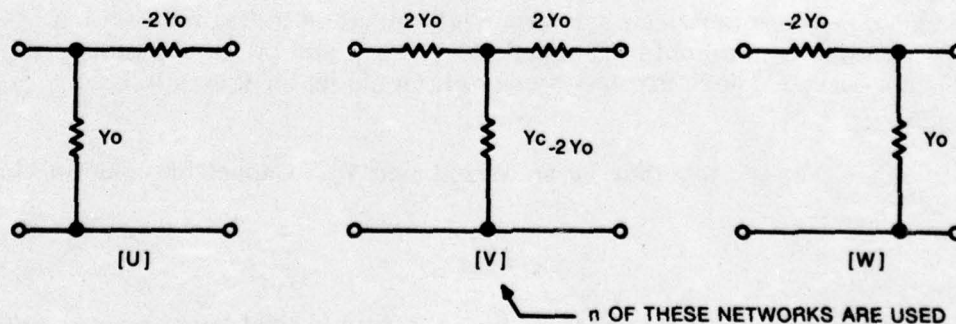


Figure 2.2-3. Filter With n Resonators, Resultant Equivalent Circuit.

Using ABCD matrices, U, V, and W become:

$$U = \begin{bmatrix} 1 & 0 \\ Y_0 & 1 \end{bmatrix} \begin{bmatrix} 1 & -\frac{1}{2Y_0} \\ 0 & 1 \end{bmatrix} = \begin{bmatrix} 1 & -\frac{1}{2Y_0} \\ Y_0 & 1/2 \end{bmatrix}$$

$$V = \begin{bmatrix} 1 & \frac{1}{2Y_0} \\ 0 & 1 \end{bmatrix} \begin{bmatrix} 1 & 0 \\ Y_c - 2Y_0 & 1 \end{bmatrix} \begin{bmatrix} 1 & \frac{1}{2Y_0} \\ 0 & 1 \end{bmatrix} = \begin{bmatrix} \frac{Y_c}{2Y_0} & \frac{1}{2Y_0} + \frac{Y_c}{4Y_0^2} \\ Y_c - 2Y_0 & \frac{Y_c}{2Y_0} \end{bmatrix}$$

$$W = \begin{bmatrix} 1 & -\frac{1}{2Y_0} \\ 0 & 1 \end{bmatrix} \begin{bmatrix} 1 & 0 \\ Y_0 & 1 \end{bmatrix} = \begin{bmatrix} 1/2 & -\frac{1}{2Y_0} \\ Y_0 & 1 \end{bmatrix}$$

The complete network matrix is:

$$X = UV^nW$$

Examining the matrix V,

$$\text{Det } V = AD - BC = \left(\frac{Y_c}{2Y_0}\right)^2 - (Y_c - 2Y_0)\left(\frac{1}{2Y_0} + \frac{Y_c}{4Y_0^2}\right) = 1$$

Thus, by the Cayley Hamilton Theorem, V^n may be written as:

$$V^n = S_1 V - S_2$$

where:

$$S_1 = \frac{\sin n\Theta}{\sin \Theta}, S_2 = \frac{\sin (n-1)\Theta}{\sin \Theta}, \text{Cos } \Theta = \frac{Y_c}{2Y_0}$$

Thus:

$$X = UV^n W = S_1 UVW - S_2 UW$$

$$X = S_1 \begin{bmatrix} 1 & -\frac{1}{2Y_0} \\ Y_0 & \frac{1}{2} \end{bmatrix} \begin{bmatrix} \frac{Y_c}{2Y_0} & \frac{1}{2Y_0} + \frac{Y_c}{4Y_0^2} \\ Y_c - 2Y_0 & \frac{Y_c}{2Y_0} \end{bmatrix} \begin{bmatrix} \frac{1}{2} & -\frac{1}{2Y_0} \\ Y_0 & 1 \end{bmatrix}$$

$$-S_2 \begin{bmatrix} 1 & -\frac{1}{2Y_0} \\ Y_0 & \frac{1}{2} \end{bmatrix} \begin{bmatrix} \frac{1}{2} & -\frac{1}{2Y_0} \\ Y_0 & 1 \end{bmatrix}$$

$$X = S_1 \begin{bmatrix} 1 & \frac{1}{2Y_0} \\ Y_c - Y_0 & \frac{1}{2} + \frac{Y_c}{2Y_0} \end{bmatrix} \begin{bmatrix} \frac{1}{2} & -\frac{1}{2Y_0} \\ Y_0 & 1 \end{bmatrix} - S_2 \begin{bmatrix} 0 & -\frac{1}{Y_0} \\ Y_0 & 0 \end{bmatrix}$$

$$X = S_1 \begin{bmatrix} 1 & 0 \\ Y_c & 1 \end{bmatrix} - S_2 \begin{bmatrix} 0 & -\frac{1}{Y_0} \\ Y_0 & 0 \end{bmatrix} = \begin{bmatrix} S_1 & \frac{S_2}{Y_0} \\ S_1 Y_c - S_2 Y_0 & S_1 \end{bmatrix}$$

The insertion loss of a network in terms of the ABCD parameters is:

$$L = 10 \log \frac{1}{4} \left| A + D + BG_t + \frac{C}{G_t} \right|^2$$

Therefore:

$$L = 10 \log \frac{1}{4} \left| \left(2 + \frac{Y_c}{G_t} \right) S_1 + \left(\frac{G_t}{Y_0} - \frac{Y_0}{G_t} \right) S_2 \right|^2$$

The loss in the stopband (L_s) is found from the above equation by assuming that the dissipation loss of the filter offers negligible loss as compared to the selectivity loss; that is, the unloaded Q is infinite.

Thus:

$$Y_c = j2G_t Q_t U$$

$$Y_o = jG_t$$

$$\cos \theta = Q_t U$$

The stopband loss is:

$$LS = 10 \log \frac{1}{4} \left| (2 + j2Q_t U) \frac{\sin n\theta}{\sin \theta} - j2 \frac{\sin (n-1)\theta}{\sin \theta} \right|^2$$

$$LS = 10 \log \left[1 - \sin^2 n\theta + \frac{\sin^2 n\theta}{\sin^2 \theta} \right]$$

$$LS = 10 \log \left[\frac{1 - \cos^2 \theta \cos^2 n\theta}{1 - \cos^2 \theta} \right]$$

The stopband loss may be written as:

$$L_s = 10 \log \frac{1 - a^2 T_n^2(a)}{1 - a^2} \quad \text{where: } a = Q_t U$$

and: $T_n(a)$ is the Tchebycheff polynomial of the first kind.

The above equation gives the stopband attenuation for the minimum loss filter employing any number (n) of resonators. Expansion of the equation results in the following expressions for various values of n :

$$n = 1, L_s = 10 \log \frac{1}{4} [b^2 + 4]$$

$$n = 2, L_s = 10 \log \frac{1}{4} [b^4 + 4]$$

$$n = 3, L_s = 10 \log \frac{1}{4} [b^2 (b^2 - 1)^2 + 4]$$

$$n = 4, L_s = 10 \log \frac{1}{4} [b^4 (b^2 - 2)^2 + 4]$$

$$n = 5, L_s = 10 \log \frac{1}{4} [b^2 (b^4 - 3b^2 + 1)^2 + 4]$$

$$n = 6, L_s = 10 \log \frac{1}{4} [b^4 (b^4 - 4b^2 + 3)^2 + 4]$$

Where: $b = 2Q_t U$

For the specified vhf filter, $L_S = 40$ dB, and $U = 0.05$, corresponding to a 5-percent frequency spacing. The required terminal Q to achieve this selectivity is computed from the previous equations and shown in table 2.2-1.

Table 2.2-1. Terminal Q Versus Number of Resonators.

N	Qt
1	2000.0
2	141.4
3	59.0
4	40.2
5	31.0
6	27.0

The loss in the passband (L_O) is found from the general loss expression when the circuit is resonant at the operating frequency, $U = 0$. For this case the equations become:

$$Y_C = G_t \left(\frac{Q_t}{Q_u} \right)$$

$$Y_O = jG_t \sqrt{1 + \frac{Q_t}{Q_u}}$$

$$\cos \theta = \frac{Q_t/Q_u}{j2 \sqrt{1 + \frac{Q_t}{Q_u}}}$$

$$L_O = 10 \log \frac{1}{4} \left(2 + \frac{Q_t}{Q_u} \right)^2 \left| S_1 + \frac{S_2}{j \sqrt{1 + \frac{Q_t}{Q_u}}} \right|^2$$

The passband loss expression may be simplified to read:²

$$L_o = 10 \log \frac{1}{4} \left(2 + \frac{Q_t}{Q_u} \right)^2 \left(1 + \frac{Q_t}{Q_u} \right)^{n-1}$$

A very useful approximation for $L_o < 2n$ dB is:

$$L_o = 10 n \log \left(1 + \frac{Q_t}{Q_u} \right)$$

The volume occupied by a helical resonator filter is approximately:

$$V = 1.6 nS^3$$

Where: S is the dimension of one side of the resonator in inches.

In the case of the deliverable hardware:

$$n = 3, S = 2.25 \text{ inches}, V = 54.675 \text{ in}^3.$$

Holding the filter volume constant, the S dimension versus n is given in table 2.2-2.

Table 2.2-2. S-Dimension Versus Number of Resonators for a Total Filter Volume of 54.675 In³.

n	S (inches)
1	3.25
2	2.58
3	2.25
4	2.05
5	1.90
6	1.79

The unloaded Q (Q_u) of each resonator is the parallel combination of the helix unloaded Q (Q_H) and the tuning capacitor Q (Q_C):

$$Q_u = \frac{Q_H Q_C}{Q_H + Q_C}$$

The tuning capacitor Q is assumed to be 5,000. The Q of the helix is given by:

$$Q_H = 60 S \sqrt{f_o}$$

Where f_o is the lowest operating frequency in MHz. The lowest operating frequency results in the worst case efficiency for the filter, thus:

$$Q_u = \frac{1650 S}{5 + 0.33 S}$$

Using the values of S given in table 2.2-2 results in table 2.2-3.

Table 2.2-3. Resonator Unloaded Q for a 54.675-In³ Filter.

n	Q _u
1	883
2	728
3	647
4	596
5	557
6	528

Using the value of Q_u from table 2.2-3 and the value of Q_t from table 2.2-1, the insertion loss of the filter at resonance is given in table 2.2-4.

Table 2.2-4. Insertion Loss Versus the Number of Resonators for a Minimum Loss Filter of $54.675 \ln^3$, Having 40 dB of Attenuation 5 Percent From the Operating Frequency.

n	L_0 , dB
1	5.139
2	1.542
3	1.137
4	1.134
5	1.176
6	1.300

The data in table 2.2-4 is plotted in figure 2.2-4. It can be seen that a 3-resonator filter provides the best performance and least complexity for the given design constraints.

The results of this section shows that a filter employing 3 resonators ($n = 3$) gives the most efficient design. The terminal Q (Q_t) should have a value of 59. The terminal Q should be held as constant as possible over the filters operating frequency range, so as to maintain a constant percentage bandwidth.

The value of the coupling coefficient (used for internal aperture design) should have a constant value of:

$$k = \frac{1}{Q_t} \sqrt{1 + \frac{Q_t}{Q_u}} \approx \frac{1}{Q_t} = \frac{1}{59} = 0.01695$$

2.3 OUTPUT COUPLING

The output coupling must load the output resonator to a nearly constant terminal Q (Q_t) as the filter is tuned from 30 to 80 MHz. The coupling must possess sufficient physical length to allow up to 10 filters to be grouped around the common junction point. The coupling must be such that the shunting reactance of the off-channel branches has a reasonable value with respect to the on-channel resistive component at the junction.

Preliminary calculation indicated that the above conditions might be met by using a transmission line for the output coupling element, provided the line is used as an impedance transformer to give the proper reactance to resistance ratio at the junction. If a transmission line having a Z_0 of 50 ohms is employed, the impedance level coupled into the output resonator must be in excess of 500 ohms. Laboratory investigation showed that the desired terminal Q (59) could not be achieved with loop coupling at the 500-ohm level. Tap coupling, however, could provide the proper loading. The total junction impedance is shown in figure 2.3-1.

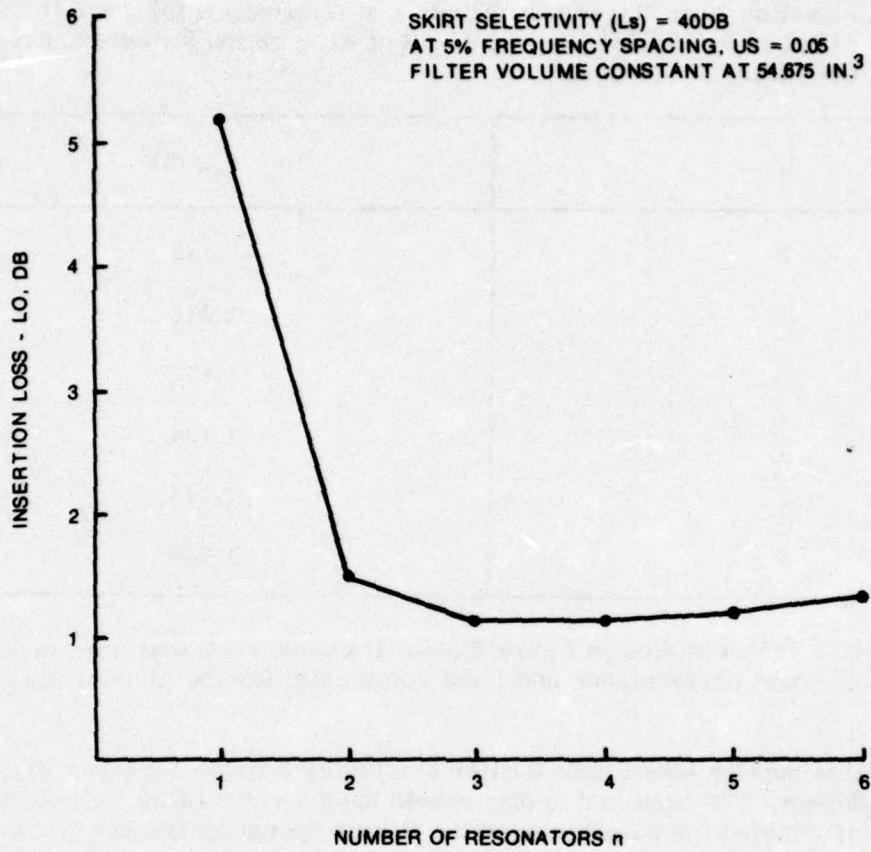


Figure 2.2-4. Number of Resonators Versus Insertion Loss.

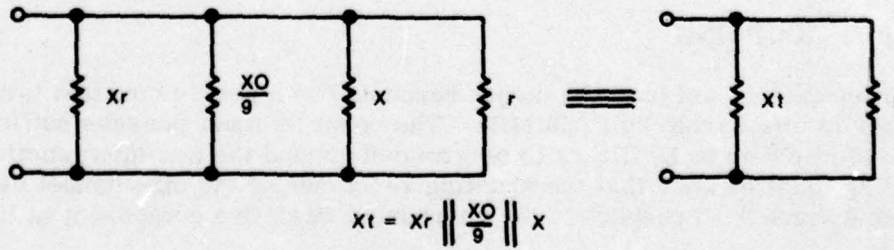


Figure 2.3-1. Total Junction Impedance.

The total impedance is composed of four elements in parallel. X_0 represents the reactance of an off-channel branch. Since one of the channels of the multicoupler is on frequency in this analysis, the remaining nine channels form a total shunting reactance of $X_0/9$. Note that the limiting case junction problem occurs for the multicoupler configuration containing the highest number of channels, that is, ten. Thus, the analysis is performed for this case. An approximate equivalent circuit of an off-channel branch is shown in figure 2.3-2.

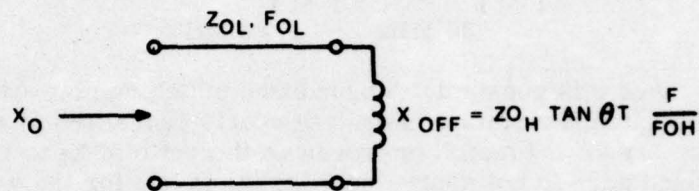


Figure 2.3-2. Equivalent Circuit of an Off-Channel Branch.

The circuit consists of a connecting transmission line having a characteristic impedance of Z_{OL} and a quarter-wave resonant frequency of f_{OL} . The line is terminated in the off-channel impedance of the filter (X_{OFF}). This off-channel filter impedance is assumed to be the portion of the helical output resonator from the tap point θ_t to ground, the helical resonator having a characteristic impedance of Z_{OH} and a self-resonant frequency of f_{OH} . Again, laboratory measurements confirmed that approximating X_{OFF} in this manner is a fairly valid assumption.

The on-channel branch gives two components to the total junction impedance, namely, X and r , where X is the residual reactance presented at the junction and r is the resistive component at the junction. The equivalent circuit of the on-channel branch is shown in figure 2.3-3.

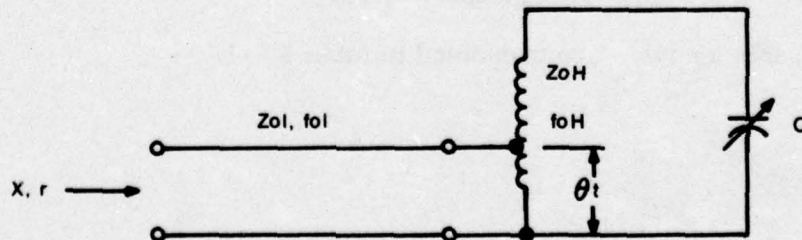


Figure 2.3-3. Equivalent Circuit of an On-Channel Branch.

The circuit consists of a connecting transmission line (identical to those in the off-channel branches) tapped into the output resonator at θ_t . Capacitor C tunes the output resonator to the on-channel frequency.

A compensating reactance (X_r) is added to the junction so as to resonate the junction at the mean of the 30- to 80-MHz band. In this case a capacitor is required to resonate the junction since the transmission lines and X_{off} are inductive. The compensating capacitor (C_r) is selected so that:

$$\left| X_t \right|_{30 \text{ MHz}} = \left| X_t \right|_{80 \text{ MHz}}$$

The junction resistance r is constant. A broadband matching network connected between the junction and the antenna terminal is used to nearly cancel the junction reactance. The effectiveness of the broadband match improves as the ratio of X_t to r increases. If the X_t/r ratio at the band edge is not appreciably less than one for the worst case (10-channel multicoupler) an efficient match may be obtained.³ If a suitable X_t/r ratio can be achieved for the 10-channel case, the ratio will be significantly better for multicouplers using less than 10 channels.

A computer program was written to optimize the output network. Given the following requirements:

- a. r is a constant
- b. $\left| X_t \right|/r$ evaluated at the band edges must be greater than 1
- c. Q_t as flat as possible with a minimum value of 59
- d. $\left| X_t \right|_{30 \text{ MHz}}$ equal to $\left| X_t \right|_{80 \text{ MHz}}$
- e. Z_{oL} equal 50 ohms.

Find the following parameters:

- a. The characteristic impedance of the helical resonator (Z_{oH})
- b. The self-resonant frequency of the helical resonator (f_{oH})
- c. The quarter-wave resonant frequency of the connecting line (f_{oL})
- d. The value of r
- e. The angular position of the tap point (θ_t)
- f. The value of the compensating capacitor (C_r)

The results of this analysis are presented in table 2.3-1.

Table 2.3-1. Optimum Parameters for Output Coupling Circuit.

ELEMENT	VALUE
Z_{OH}	295.7 ohms
f_{OH}	99.0 MHz
f_{OL}	105.2 MHz
r	6.9956 ohms
θ_t	17.933 degrees
Cr	79.98 pF

The analysis includes resonator and connecting line loss. The variation in Q_t was computed to vary from 59 to 72. The value of $|X_t|/r$ at the band edge is 1.03. It was also noted that the reactance of the on-channel (X) may be neglected compared to the reactance of the off channels (X_O). Using the value of f_{OL} , the physical length of the connecting transmission lines with a Teflon dielectric is 19.95 inches, which is more than adequate to permit filter interconnection.

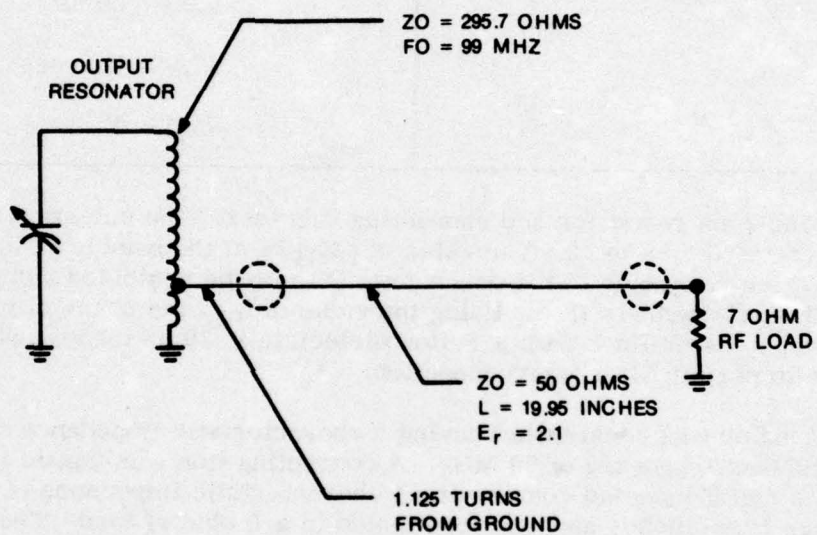
An output resonator was constructed having a characteristic impedance of 295.7 ohms and a self-resonant frequency of 99 MHz. A connecting line was tapped into the helix. The line was a metal jacketed coax having a characteristic impedance of 50 ohms. The line length was 19.95 inches and was terminated in a 7-ohm rf load. The tap point was adjusted to give the best terminal Q characteristics. Figure 2.3-4 gives the results of this measurement.

The resonant frequency of the connecting line (f_{OL}) was measured to be 102 MHz. The connecting line was removed from the resonator and the reactance looking into the resonator at the tap (X_{off}) was measured.

$$X_{off30 \text{ MHz}} = +j 14.3 \text{ ohms}$$

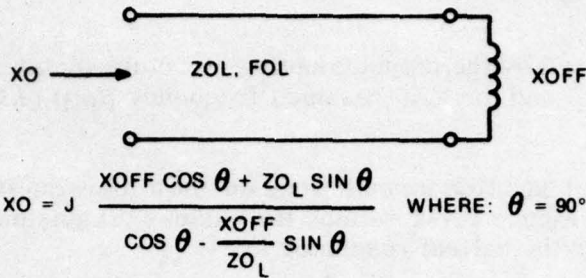
$$X_{off80 \text{ MHz}} = +j 61.0 \text{ ohms}$$

The measured value of (f_{OL}) and (X_{off}) were then used to recompute the value of (Cr). This computation is shown in figure 2.3-5. Also shown is the final value of $|x_t|/r$ for 2, 5, and 10-channel multicouplers. As can be seen Cr should have a value of 14 pF for each off-channel branch in the multicoupler. The $|x_t|/r$ or the x/r ratio (δ) has a minimum value of 0.826 for 10 channels and a maximum value of 7.432 for 2 channels.



F MHZ	QT
30	60.8
40	71.6
50	75.3
55	74.6
60	73.4
70	67.0
80	57.1

Figure 2.3-4. Measured Output Terminal Q.

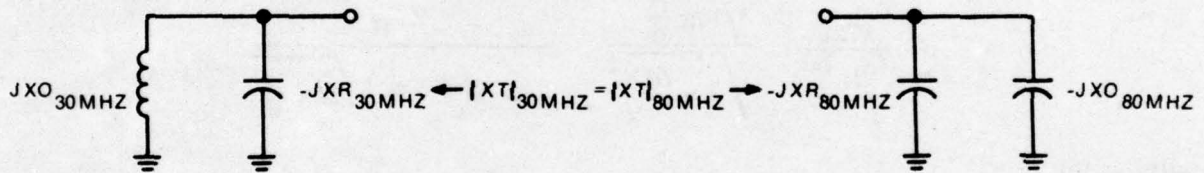


AT: 30 MHZ, $ZOL = 50 \Omega$, $XOFF = 14.3 \Omega$, $FO_L = 102 \text{ MHZ}$, $\theta = 26.47^\circ$

$$XO_{30\text{MHZ}} = J \frac{14.3 \cos 26.47^\circ + 50 \sin 26.47^\circ}{\cos 26.47^\circ - \frac{14.3}{50} \sin 26.47^\circ} = +J 45.705 \Omega$$

AT: 80 MHZ, $ZOL = 50 \Omega$, $XOFF = 61.0 \Omega$, $FO_L = 102 \text{ MHZ}$, $\theta = 70.59^\circ$

$$XO_{80\text{MHZ}} = J \frac{61.0 \cos 70.59^\circ + 50 \sin 70.59^\circ}{\cos 70.59^\circ - \frac{61.0}{50} \sin 70.59^\circ} = -J 82.395 \Omega$$



$$\text{WHERE: } CR = \frac{1}{\omega_{30\text{MHZ}} X_{R_{30\text{MHZ}}}} = \frac{1}{\omega_{80\text{MHZ}} X_{R_{80\text{MHZ}}}}$$

$$|XTI| = \frac{XO_{30\text{MHZ}} X_{R_{30\text{MHZ}}}}{X_{R_{30\text{MHZ}}} - XO_{30\text{MHZ}}} = \frac{XO_{80\text{MHZ}} X_{R_{80\text{MHZ}}}}{X_{R_{80\text{MHZ}}} + XO_{80\text{MHZ}}}$$

$$CR = \frac{XO_{80\text{MHZ}} - XO_{30\text{MHZ}}}{(\omega_{30\text{MHZ}} + \omega_{80\text{MHZ}}) XO_{80\text{MHZ}} XO_{30\text{MHZ}}} = \frac{82.395 - 45.705}{(2\pi \times 30 \times 10^6 + 2\pi \times 80 \times 10^6) (82.395) (45.705)} = 14.0965 \text{ PF}$$

PER CHANNEL

$$X_{R_{30\text{MHZ}}} = 376.346 \Omega, \quad X_{R_{80\text{MHZ}}} = 141.130 \Omega, \quad |XTI|_{30\text{MHZ}} = |XTI|_{80\text{MHZ}} = 52.023 \text{ OHMS PER CHANNEL}$$

$$\text{FOR: } 10 \text{ CHANNELS, } r = 7 \Omega \quad X = \frac{|XTI|}{9} = 5.780 \quad \delta_{10} = \frac{X}{r} = 0.826$$

$$\text{FOR: } 5 \text{ CHANNELS, } r = 7 \Omega \quad X = \frac{|XTI|}{4} = 13.006 \quad \delta_5 = \frac{X}{r} = 1.858$$

$$\text{FOR: } 2 \text{ CHANNELS, } r = 7 \Omega \quad X = \frac{|XTI|}{1} = 52.023 \quad \delta_2 = \frac{X}{r} = 7.432$$

Figure 2.3-5. Output Coupling Computations.

2.4 RESONATOR DESIGN

The requirements imposed by the output coupling structure dictates that the characteristic impedance (Z_{OH}) and the self-resonant frequency (f_{OH}) of the helix both be controlled.

Existing nomographs and equation formulations do not allow simultaneous control of these two parameters. Figure 2.4-1 defines the various dimensions of the resonator. The design equations for the helical resonator are⁴:

$$n = \frac{1720}{f_{OH} bd} \cdot \frac{\sqrt{\log \frac{D}{d}}}{\sqrt{1 - \left(\frac{d}{D}\right)^2}} \quad \text{and:} \quad Z_{OH} = 183 nd \left(1 - \frac{d}{D}\right) \sqrt{\log \frac{D}{d}}$$

Where:

$$D = 1.2 S \text{ and } n \text{ is in turns per inch.}$$

Eliminating n:

$$n = \frac{1720}{f_{OH} bd} \cdot \frac{\sqrt{\log \frac{D}{d}}}{\sqrt{1 - \left(\frac{d}{D}\right)^2}} = \frac{Z_{OH}}{183 d \left(1 - \frac{d}{D}\right) \sqrt{\log \frac{D}{d}}}$$

Solving for b:

$$b = \frac{(314760) \left(1 - \frac{d}{D}\right) \log \frac{D}{d}}{f_{OH} Z_{OH} \sqrt{1 - \left(\frac{d}{D}\right)^2}}$$

The equations are most accurate when $b/d = 1.5$, therefore:

$$df_{OH} Z_{OH} \sqrt{1 - \left(\frac{d}{D}\right)^2} = (209840) \left(1 - \frac{d}{D}\right) \log \frac{D}{d}$$

For the particular problem at hand:

$$f_{OH} = 99 \text{ MHz}$$

$$Z_{OH} = 295.7 \text{ ohms}$$

$$D = 1.2 S = (1.2) (2.25) = 2.7 \text{ inches}$$

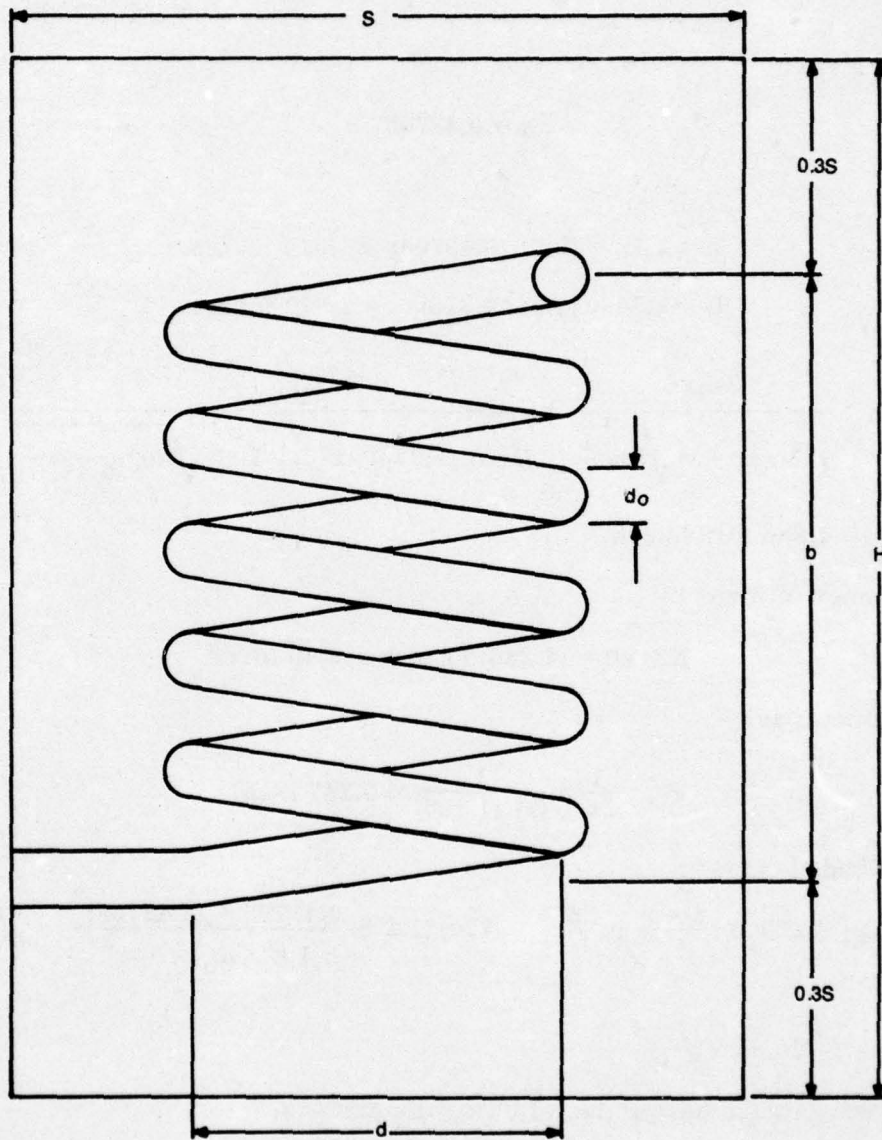


Figure 2.4-1. Helical Resonator Dimensions.

Thus:

$$x \sqrt{1 - x^2} = k (1 - x) \log \frac{1}{x} \quad x = \frac{d}{2.7}$$
$$k = 2.654838$$

Solving for x gives:

$$x = 0.48708$$

Then:

$$d = 2.7x = (2.7) (0.48708) = 1.315 \text{ inches}$$

$$b = 1.5d = (1.5) (1.315) = 1.973 \text{ inches}$$

$$n = \frac{Z_{oH}}{183d (1 - x) \sqrt{\log \frac{1}{x}}} = \frac{295.7}{(183) (1.315) (1 - 0.48708) \sqrt{\log \frac{1}{0.48708}}}$$
$$= 4.286 \text{ turns/inch}$$

The total number of turns is:

$$N = nb = (4.286) (1.973) = 8.45 \text{ turns}$$

The wire diameter is:

$$d_o = \frac{1}{2n} = \frac{1}{(2) (4.286)} = 0.117 \text{ inch}$$

The helix unloaded Q is:

$$Q_H = 220 D \frac{x - x^3}{1.5 - x^3} \sqrt{f_o} = (220) (1.2 S) \frac{0.48708 - (0.48708)^3}{1.5 - (0.48708)^3} \sqrt{f_o}$$
$$= 70.85 S \sqrt{f_o}$$

A helix was constructed having the following dimensions:

$$S = 2.25 \text{ inches}$$

$$d_o = 0.125 \text{ inches}$$

$$d = 1.312 \text{ inches}$$

$$N = 8.4 \text{ turns}$$

With no dielectric support on the helix the self-resonant frequency was measured as 98.811 MHz and the measured value of Q_{II} was 1235. When the dielectric support was installed the total number of turns on the helix was reduced to 7.625 to preserve the resonant frequency of 99 MHz. Measured Q_{II} at 99 MHz for the helix with support was 1223.

The helix is tuned to the operating frequency range by means of a gas filled variable capacitor. The minimum capacity is given by:

$$C_{\min} = \frac{10^6}{2\pi f_{\max} Z_{oH} \tan\left(90^\circ \frac{f_{\max}}{f_{oH}}\right)} = \frac{10^6}{(2\pi)(80)(259.7) \tan\left(90^\circ \frac{80}{99}\right)} = 2.382 \text{ pF}$$

The maximum required capacity is:

$$C_{\max} = \frac{10^6}{2\pi f_{\min} Z_{oH} \tan\left(90^\circ \frac{f_{\min}}{f_{oH}}\right)} = \frac{10^6}{(2\pi)(30)(259.7) \tan\left(90^\circ \frac{30}{99}\right)} = 39.625 \text{ pF}$$

The range of the gas filled variable capacitor as employed in the deliverable hardware has a capacity range of 1.5 to 45 pF.

The maximum capacitor voltage must be calculated using the resonator reactance slope parameter (χ) to obtain the equivalent inductive resistance (X_{Le}).

At 30 MHz:

$$\theta_o = 90^\circ \frac{F}{f_{oH}} = 90^\circ \frac{30}{99} = 27.273^\circ = 0.476 \text{ radians}$$

$$\chi = \frac{1}{2} + \frac{\theta_o}{\sin 2\theta_o} = 0.5 + \frac{0.476}{\sin 54.545^\circ} = 1.084$$

$$X_{Le} = \frac{Z_{oH} \tan \theta_o}{\chi} = \frac{259.7 \tan 27.273^\circ}{1.084} = 123.51 \text{ ohms}$$

At 80 MHz:

$$\theta_o = 90^\circ \frac{f}{f_{oH}} = 90^\circ \frac{80}{99} = 72.727^\circ = 1.269 \text{ radians}$$

$$\chi = \frac{1}{2} + \frac{\theta_o}{\sin 2\theta_o} = 0.5 + \frac{1.269}{\sin 145.454^\circ} = 2.738$$

$$X_{Le} = \frac{Z_{oH} \tan \theta_o}{\chi} = \frac{295.7 \tan 72.727^\circ}{2.738} = 347.33 \text{ ohms}$$

The peak capacitor voltage is:

$$E_p = \sqrt{2PQ_t X_{L_c}} \quad P = 60 \text{ watts}$$

$$\text{At 30 MHz: } E_p = \sqrt{(2)(60)(59)(123.51)} = 935.12 \text{ volts}$$

$$\text{At 80 MHz: } E_p = \sqrt{(2)(60)(59)(347.33)} = 1568.15 \text{ volts}$$

The gas filled variable capacitor as employed in the deliverable hardware has a minimum rf voltage rating of 3000 volts. The capacitor rms current is found from:

$$I_c = \frac{E_p}{\sqrt{2} X_c}$$

At 30 MHz:

$$I_c = \frac{935.12}{\sqrt{2} \left[\frac{10^6}{2\pi(30)(39.625)} \right]} = 4.939 \text{ amperes}$$

At 80 MHz:

$$I_c = \frac{1568.15}{\sqrt{2} \left[\frac{10^6}{2\pi(80)(2.382)} \right]} = 1.328 \text{ amperes}$$

The gas filled variable capacitor is rated at 15 amperes.

The helix surface area is:

$$A = \pi db = \pi (1.315)(1.973) = 8.15 \text{ square inches}$$

The power dissipated in each resonator is approximately:

$$P_d = \frac{P}{n} \left(1 - \frac{1}{10 \left(\frac{L_o}{10} \right)} \right) = \frac{60}{3} \left(1 - \frac{1}{10 \left(\frac{1.137}{10} \right)} \right) = 4.606 \text{ watts}$$

This results in a power density on the surface of the helix of

$$\frac{4.606}{8.15} = 0.565 \text{ watt/in}^2$$

This power density is well below the recommended maximum of 1 watt per square inch.

The complete resonator (helix, dielectric support, and capacitor) have a measured temperature coefficient of less than -20 ppm/ $^{\circ}\text{C}$ for a 75 $^{\circ}\text{C}$ temperature change. The measured unloaded Q (Q_u) of the resonator is given in table 2.4-1.

Table 2.4-1. Resonator Measured Unloaded Q.

F_o , MHz	Q_u
30	671.3
40	756.2
50	821.1
60	847.5
70	869.6
80	884.0

2.5 MATCHING NETWORK DESIGN

From paragraph 2.3, the design of the output coupling structure required an rf load resistance (r) of 7 ohms to achieve a suitable x/r ratio at the multicoupler common junction point.

The matching network design is thus divided into two distinct tasks. One, a broadband impedance transformation network to translate a 7-ohm resistive load to a 50-ohm resistive load (antenna impedance). And, two, a reactance canceling network to optimize the vswr across the operating frequency range.

A network is used for the resistance transformation rather than a broadband iron core transformer because of the nonlinearities common to the transformer design. IMD and harmonic distortion would be severe in an iron core design since the network must handle as high as 600 watts in the 10-channel case. The word "transformer" is used in this discussion as a matter of convenience and refers to a network that provides impedance transformation.

The transformer is derived from a bandpass filter design having Tchebycheff characteristics. The passband width must be at least 50 MHz wide; for example, the transformer must operate from 30 to 80 MHz. The input impedance is 7 ohms when the output is terminated in 50 ohms over the passband width. Selectivity of the network is immaterial. The transformer action is incorporated into the network by repeated use of Norton's first transformation as shown in figure 2.5-1.

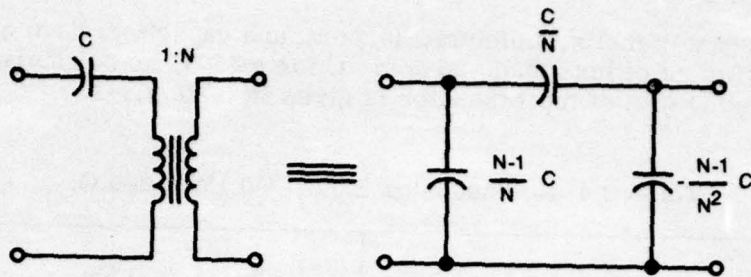


Figure 2.5-1. Norton's First Transformation.

Preliminary calculations indicated that a 4-pole network ($n = 4$) would be required to achieve a good match over the required frequency range.

The initial form of the network and the transformations are depicted in figure 2.5-2. The last circuit in figure 2.5-2 shows the final form of the transformer. The next step is to evaluate the elements comprising the network. Since a good match is desired across the frequency range, a low vswr Tchebycheff prototype is selected. Let the passband ripple (L_{Ar}) be 0.01 dB, this corresponds to a vswr of 1.1:1. The g parameters are:⁵

$$g_0 = 1.0000, g_1 = 0.7128, g_2 = 1.2003, g_3 = 1.3212, g_4 = 0.6476$$

$$g_5 = 1.1007, \omega_1' = 1.0000, L_{Ar} = 0.01 \text{ dB}, n = 4$$

It is also known that:

$$R_o = r = 7 \text{ ohms}, N^4 R_5 = 50 \text{ ohms}$$

Also:

$$N^4 R_5 = N^4 R_o g_5 = 50$$

The equivalent transformer turns ratio (N) is therefore:

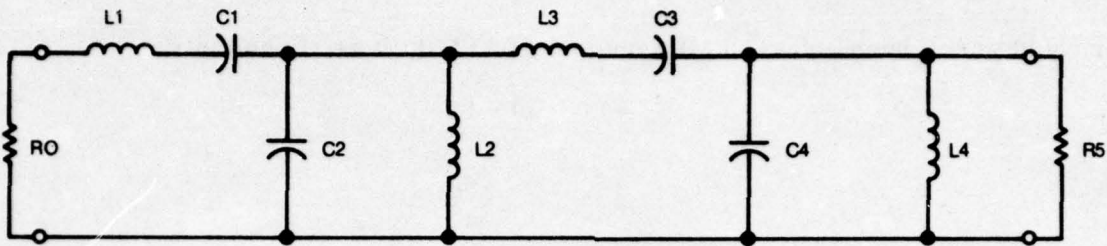
$$N = \left(\frac{50}{R_o g_5} \right)^{\frac{1}{4}} = \left[\frac{50}{(7)(1.1007)} \right]^{\frac{1}{4}} = 1.596066$$

From figure 2.5-2 the fractional bandwidth (w) may be found as:

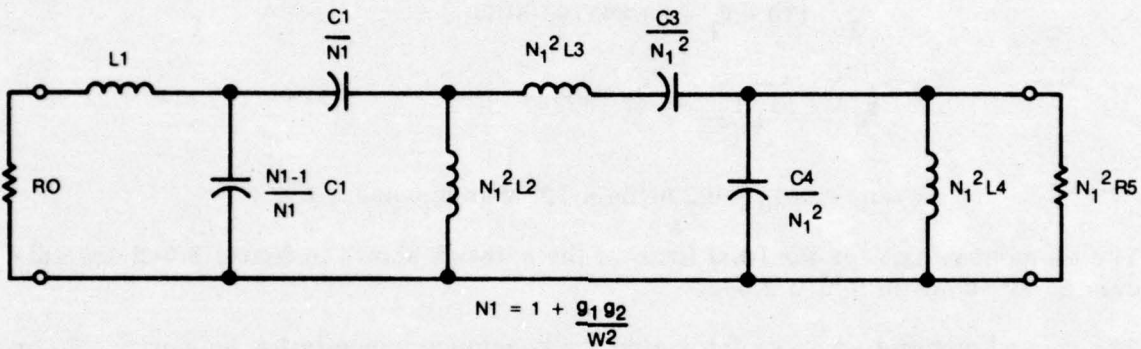
$$w = \sqrt{\frac{g_1 g_2}{N-1}} = \sqrt{\frac{(0.7128)(1.2003)}{0.596066}} = 1.198068$$

Also:

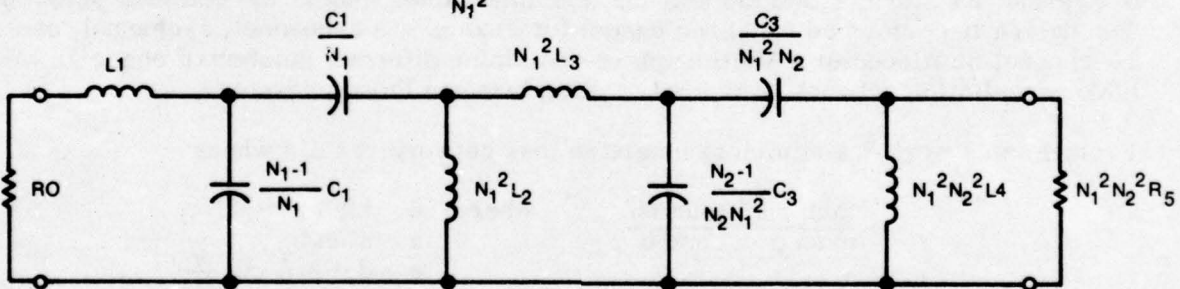
$$w = \frac{f_2 - f_1}{f_o} = \frac{f_2 - f_1}{\sqrt{f_1 f_2}}$$



APPLY NORTON'S TRANSFORMATION TO C_1 , SUCH THAT C_2 IS ABSORBED:



APPLY NORTON'S TRANSFORMATION TO $\frac{C_3}{N_1^2}$, SUCH THAT $\frac{C_4}{N_1^2}$ IS ABSORBED:



FOR A TCHEBYCHEFF DESIGN IT IS KNOWN THAT: $g_1 g_2 = g_3 g_4$. THEREFORE $N_1 = N_2 = N$.

THUS:

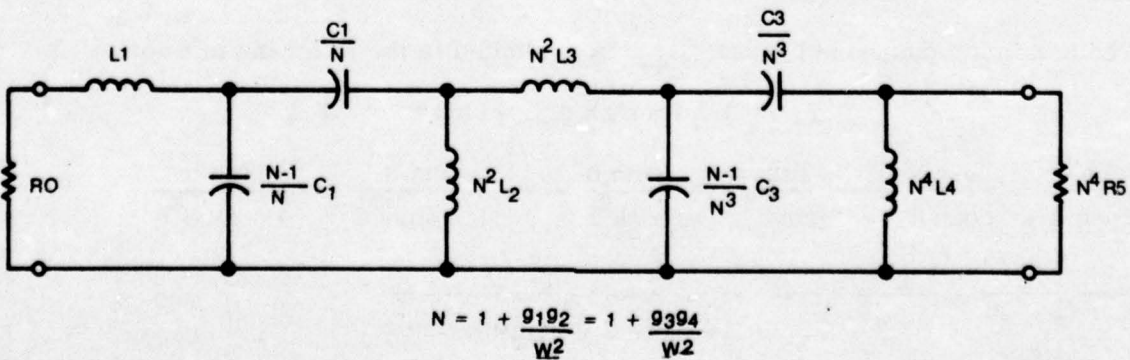


Figure 2.5-2. Reduction of Transformer to Final Form.

For equal guardbands above 80 MHz and below 30 MHz it requires that:

$$f_2 - 80 = 30 - f_1$$

Thus:

$$f_1 = 55 \left(1 - \frac{w}{\sqrt{4 + w^2}} \right) = 26.736254 \text{ MHz}$$

$$f_2 = 110 - f_1 = 83.263746 \text{ MHz}$$

$$f_0 = \sqrt{f_1 f_2} = 47.182207 \text{ MHz}$$

$$\omega_0 = 2\pi f_0 = 0.296454 \times 10^9 \text{ radians/second.}$$

The element values for the final form of the network shown in figure 2.5-2 are calculated as shown in figure 2.5-3.

The second design task is to determine the reactance cancellation networks. To provide reasonable element values, the cancellation networks are inserted between the *broadband transformer* and the *antenna terminal* rather than at the common junction. The design is performed for three cases; for example, a 2-channel, 5-channel, and a 10-channel multicoupler. Multicouplers containing different number of channels would have cancellation network complexity falling between those presented.

From Fano's work,⁶ a minimum insertion loss network results when:

$$\frac{\tanh na}{\cosh a} = \frac{\tanh nb}{\cosh b} \quad \text{where: } d = \sinh a$$

$$e = \sinh b$$

$$e = d - 2\delta \sin \frac{\pi}{2n}$$

In the above equations n is the number of elements comprising the low-pass prototype network. $n = 1$ is the case where no matching network is required. δ is the x/r ratio evaluated at the band edges.

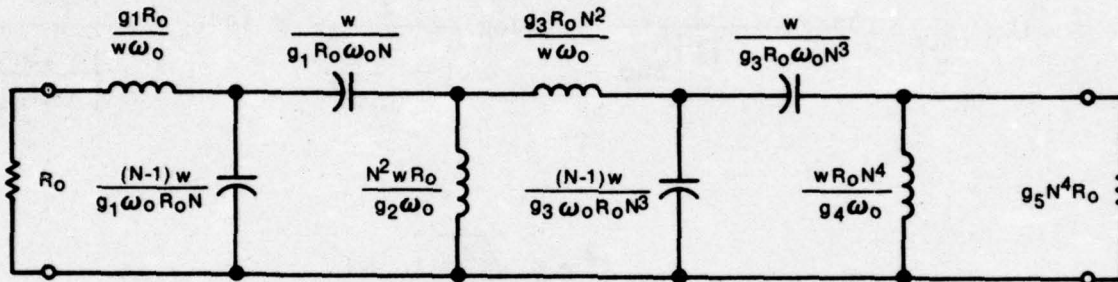
The maximum passband loss $(L_A)_{\max}$ is evaluated in the following manner:

$$\text{For, } n = 1: d = \sinh a, e = \sinh b, e = d - 2\delta$$

$$\frac{\tanh a}{\cosh a} = \frac{\tanh b}{\cosh b} \rightarrow \frac{\sinh a}{\cosh^2 a} = \frac{\sinh b}{\cosh^2 b} \rightarrow \frac{\sinh a}{1 + \sinh^2 a} = \frac{\sinh b}{1 + \sinh^2 b}$$

$$\rightarrow \frac{d}{1 + d^2} = \frac{e}{1 + e^2} \rightarrow \frac{d}{1 + d^2} = \frac{d - 2\delta}{1 + d^2 - 4\delta d + 4\delta^2}$$

THE NETWORK IN TERMS OF THE KNOWN QUANTITIES IS:



WHERE:

$$R_0 = 7 \text{ OHMS}, G_1 = 0.7128, G_2 = 1.2003, G_3 = 1.3212, G_4 = 0.6476,$$

$$G_5 = 1.1007, W = 1.198068, \omega_0 = 0.296454 \times 10^9, N = 1.598066,$$

$$N^2 = 2.547427, N^3 = 4.065861, N^4 = 6.489383.$$

THE ELEMENT VALUES ARE:

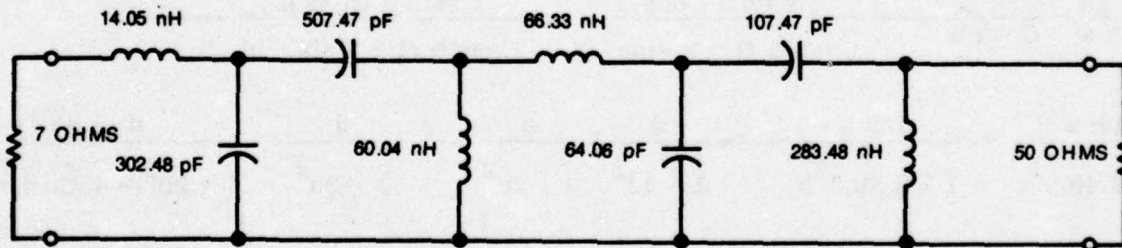


Figure 2.5-3. Transformer Element Values.

Solving for d and e in terms of δ gives:

$$d = \sqrt{\delta^2 + 1} + \delta = \sinh a$$

$$e = \sqrt{\delta^2 + 1} - \delta = \sinh b$$

Then:

$$(LA)_{\max} = 10 \log \frac{1}{1 - |\Gamma|_{\max}^2} = 10 \log \frac{1}{1 - \frac{\cosh^2 b}{\cosh^2 a}} = 10 \log \frac{1}{1 - \frac{1 + \sinh^2 b}{1 + \sinh^2 a}}$$

Or:

$$(LA)_{\max} = 10 \log \frac{\delta^2 + \delta \sqrt{\delta^2 + 1} + 1}{2\delta \sqrt{\delta^2 + 1}}$$

For, $n = 2$:

$$d = \sinh a, e = \sinh b, e = d - \sqrt{2}\delta$$

$$\frac{\tanh 2a}{\cosh a} = \frac{\tanh 2b}{\cosh b} \rightarrow \frac{2 \sinh a \cosh a}{\cosh a (1 + 2 \sinh^2 a)} = \frac{2 \sinh b \cosh b}{\cosh b (1 + 2 \sinh^2 b)} \rightarrow$$

$$\frac{\sinh a}{1 + 2 \sinh^2 a} = \frac{\sinh b}{1 + 2 \sinh^2 b} \rightarrow \frac{d}{1 + 2d^2} = \frac{e}{1 + 2e^2} \rightarrow \frac{d}{1 + 2d^2} = \frac{d - \sqrt{2}\delta}{1 + 2d^2 - 4\sqrt{2}d\delta + 4\delta^2}$$

Solving for d and e in terms of δ gives:

$$d = \frac{1}{\sqrt{2}} (\sqrt{\delta^2 + 1} + \delta) = \sinh a$$

$$e = \frac{1}{\sqrt{2}} (\sqrt{\delta^2 + 1} - \delta) = \sinh b$$

Then:

$$(L_A)_{\max} = 10 \log \frac{1}{1 - |\Gamma|_{\max}^2} = 10 \log \frac{1}{1 - \left(\frac{\cosh 2b}{\cosh 2a}\right)^2} = 10 \log \frac{1}{1 - \left(\frac{1 + 2 \sinh^2 b}{1 + 2 \sinh^2 a}\right)^2}$$

Or:

$$(L_A)_{\max} = 10 \log \frac{(\delta^2 + \delta\sqrt{\delta^2 + 1} + 1)^2}{4\delta(\delta^2 + 1)^{3/2}}$$

For, $n = 3$: $d = \sinh a$, $e = \sinh b$, $e = d - \delta$

$$\frac{\tanh 3a}{\cosh a} = \frac{\tanh 3b}{\cosh b} \rightarrow \frac{3 \sinh a + 4 \sinh^3 a}{\cosh a (4 \cosh^3 a - 3 \cosh a)} = \frac{3 \sinh b + 4 \sinh^3 b}{\cosh b (4 \cosh^3 b - 3 \cosh b)}$$

$$\rightarrow \frac{3 \sinh a + 4 \sinh^3 a}{(1 + \sinh^2 a)(1 + 4 \sinh^2 a)} = \frac{3 \sinh b + 4 \sinh^3 b}{(1 + \sinh^2 b)(1 + 4 \sinh^2 b)} \rightarrow \frac{3d + 4d^3}{(1 + d^2)(1 + 4d^2)}$$

$$= \frac{3e + 4e^3}{(1 + e^2)(1 + 4e^2)} \rightarrow \frac{3d + 4d^3}{(1 + 5d^2 + 4d^4)}$$

$$= \frac{3d - 3\delta + 4d^3 - 12\delta d^2 + 12\delta^2 d - 4\delta^3}{1 + 5d^2 - 10\delta d + 5\delta^2 + 4d^4 - 16\delta d^3 + 24\delta^2 d^2 - 16\delta^3 d + 4\delta^4}$$

Or:

$$16d^6 - 48d^5\delta + 16d^4 + 48d^4\delta^2 - 16d^3\delta^3 - 32d^3\delta + 3d^2 + 28d^2\delta^2 - 12d\delta^3 - 3d\delta - 4\delta^2 = 3$$

To find $(L_A)_{\max}$ solve the above equation for d given a value of δ . Then calculate $(L_A)_{\max}$ from:

$$(L_A)_{\max} = 10 \log \frac{(1 + d^2)(1 + 4d^2)^2}{(1 + d^2)(1 + 4d^2)^2 - [1 + (d - \delta)^2][1 + 4(d - \delta)^2]^2}$$

The maximum passband vswr for each case may be found from $(L_A)_{\max}$ as:

$$V_{\text{swr}}_{\max} = 2H - 1 + 2\sqrt{H(H - 1)}$$

Where:

$$H = 10 \frac{(L_A)_{\max}}{10}$$

For the 2-channel multicoupler:

$$\delta = \delta_2 = 7.432 \quad (\text{From figure 2.3-5), let } n = 1$$

$$(L_A)_{\max} = 10 \log \frac{\delta^2 + \delta \sqrt{\delta^2 + 1} + 1}{2 \delta \sqrt{\delta^2 + 1}} = 10 \log \frac{111.970}{111.465} = 0.0196 \text{ dB}$$

$$H = 10^{\frac{(L_A)_{\max}}{10}} = 1.004531$$

$$V_{\text{swr}}_{\max} = 2H - 1 + 2 \sqrt{H(H - 1)} = 1.144:1$$

This is an excellent match. Thus we can conclude for the 2-channel case no matching network is required, and the transformer output can be connected directly to the antenna terminal.

For the 5-channel multicoupler:

$$\delta = \delta_5 = 1.858 \quad (\text{From figure 2.3-5), let } n = 1$$

$$(L_A)_{\max} = 10 \log \frac{\delta^2 + \delta \sqrt{\delta^2 + 1} + 1}{2 \delta \sqrt{\delta^2 + 1}} = 10 \log \frac{8.3726}{7.8408} = 0.285 \text{ dB}$$

$$H = 10^{\frac{(L_A)_{\max}}{10}} = 1.067825$$

$$V_{\text{swr}}_{\max} = 2H - 1 + 2 \sqrt{H(H - 1)} = 1.6739:1$$

The vswr is quite high. Try $n = 2$

$$(L_A)_{\max} = 10 \log \frac{(\delta^2 + \delta \sqrt{\delta^2 + 1} + 1)^2}{4 \delta (\delta^2 + 1)^{3/2}} = 10 \log \frac{70.1004}{69.8172} = 0.0176 \text{ dB}$$

$$H = 10^{\frac{(L_A)_{\max}}{10}} = 1.004056$$

$$V_{\text{swr}}_{\max} = 2H - 1 + 2 \sqrt{H(H - 1)} = 1.1357:1$$

Thus it can be concluded that a single series tuned circuit (L_2 and C_2) connected between the transformer output and the antenna terminal will provide the desired degree of matching. The element values for the 5-channel matching network are computed in figure 2.5-4.

For the 10-channel multicoupler:

$$\delta = \delta_{10} = 0.826 \text{ (from figure 2.3-5), let, } n = 1$$

$$(LA)_{\max} = 10 \log \frac{\delta^2 + \delta \sqrt{\delta^2 + 1} + 1}{2\delta \sqrt{\delta^2 + 1}} = 10 \log \frac{2.7536}{2.1427} = 1.0894 \text{ dB}$$

$$H = 10^{\frac{(LA)_{\max}}{10}} = 1.2851$$

$$V_{\text{swr}}_{\max} = 2H - 1 + 2\sqrt{H(H-1)} = 2.7808:1$$

The vswr is extremely high, try $n = 2$.

$$(LA)_{\max} = 10 \log \frac{(\delta^2 + \delta \sqrt{\delta^2 + 1} + 1)^2}{4\delta (\delta^2 + 1)^{3/2}} = 10 \log \frac{7.5823}{7.2092} = 0.2191 \text{ dB}$$

$$H = 10^{\frac{(LA)_{\max}}{10}} = 1.0518$$

$$V_{\text{swr}}_{\max} = 2H - 1 + 2\sqrt{H(H-1)} = 1.5704:1$$

The vswr is still quite high, let , $n = 3$.

$$\delta = 0.8260, \delta^2 = 0.6823, \delta^3 = 0.5636$$

$$n = 2, \delta = \delta_5 = 1.858, H = 1.004056, f_1 = 30 \text{ MHz}, F_2 = 80 \text{ MHz}, R = 50 \text{ ohms}$$

$$d = \sinh \left[\frac{\ln \left(\sqrt{\frac{1}{H-1}} + \sqrt{\frac{1}{H-1} + 1} \right)}{n} \right] = \sinh \left[\frac{\ln (15.70186 + 15.73367)}{2} \right]$$

$$= \sinh 1.72397 = 2.71419$$

$$D = \frac{d}{\delta \sin \frac{\pi}{2n}} - 1 = \frac{2.71419 \sqrt{2}}{1.858} - 1 = 1.06590$$

$$\text{Letting: } g_0 = 1, \omega_1' = 1$$

$$g_1 = \frac{1}{\delta} = \frac{1}{1.858} = 0.53821$$

$$k_{12} = \sqrt{\frac{1 + (1 + D^2)\delta^2}{2}} = 2.04626$$

$$f_0 = \sqrt{f_1 f_2} = \sqrt{30 \times 80} = 48.989795 \text{ MHz}, \omega_0 = 2\pi f_0 = 0.307812 \times 10^9$$

$$g_2 = \frac{1}{g_1 (k_{12})^2} = 0.44374, g_3 = \frac{1}{D\delta g_2} = 1.13791$$

$$X_{L2} = X_{C2} = \frac{\omega_1' g_2 R}{w} = \frac{(1)(0.44374)(50)}{1.020621} = 21.73873 \text{ ohms}$$

$$L_2 = \frac{X_{L2}}{\omega_0} = \frac{21.73873}{0.307812} = 70.6234 \text{ nH}, C_2 = \frac{1}{X_{C2}\omega_0} = \frac{1000}{(21.73873)(0.307812)} = 149.44 \text{ pF}$$

Figure 2.5-4. 5-Channel Multicoupler Matching Network Element Values.

$$16d^6 - 48\delta d^5 + (16 + 48\delta^2)d^4 - (16\delta^3 + 32\delta)d^3 + (3 + 28\delta^2)d^2 - (12\delta^3 + 3\delta)d - (4\delta^2 + 3) = 0$$

Substituting the values of δ , δ^2 , and δ^3 into the above equation gives:

$$d^6 - 2.4780d^5 + 3.0469d^4 - 2.2156d^3 + 1.3815d^2 - 0.5776d - 0.3581 = 0$$

Solving for d:

$$d = 1.107185$$

$$(L_A)_{\max} = 10 \log \frac{(1 + d^2)(1 + 4d^2)^2}{(1 + d^2)(1 + 4d^2)^2 - [1 + (d - \delta)^2][1 + 4(d - \delta)^2]^2} = 10 \log \frac{77.572385}{75.702861}$$

$$= 0.10595$$

$$H = 10^{\frac{(L_A)_{\max}}{10}} = 1.024696$$

$$V_{\text{swr}}_{\max} = 2H - 1 + 2\sqrt{H(H - 1)} = 1.3675:1$$

Thus it can be concluded that a 2-pole network (a series tuned circuit L_2, C_2 and a parallel tuned circuit L_3, C_3 in shunt) connected between the transformer output and the antenna terminal will provide the desired degree of matching. The element values for the 10-channel matching network are computed in figure 2.5-5.

The final form of the combining/matching networks are shown in figure 2.5-6. Note the addition of the compensating capacitor at the common junction. This capacitor has a value of $(n - 1)C_F$ where n is the number of channels comprising the multicoupler, and C_F is equal to 14.0965 pF (from figure 2.3-5).

The actual component values used in the transformer and matching networks differ very slightly in the deliverable hardware (paragraph 3.4). This is due to two factors: one, standard value capacitors are used, and two, some compensation of inevitable stray capacity and inductance is required. The transformers were adjusted for a minimum return loss of 22.5 dB, this corresponds to a maximum vswr of 1.16:1.

$$n = 3, \delta = \delta_{10} = 0.8260, d = 1.107185, R = 50 \text{ ohms}, f_2 = 80 \text{ MHz}, f_1 = 30 \text{ MHz}$$

$$D = \frac{d}{\delta \sin \frac{\pi}{2n}} - 1 = \frac{1.107185}{(0.826)(0.5)} - 1 = 1.680835$$

$$\text{Letting: } g_0 = 1, \omega_1' = 1$$

$$g_1 = \frac{1}{\delta} = \frac{1}{0.826} = 1.210654$$

$$k_{12} = \sqrt{\frac{3}{8} \left[1 + \left(1 + \frac{D^2}{3}\right) \delta^2 \right]} = 0.933702$$

$$k_{23} = \sqrt{\frac{3}{8} \left[1 + \left(\frac{1}{3} + D^2\right) \delta^2 \right]} = 1.087715$$

$$g_2 = \frac{1}{g_1 (k_{12})^2} = 0.947465, \quad g_3 = \frac{1}{g_2 (k_{23})^2} = 0.892086$$

$$g_4 = \frac{1}{D \delta g_3} = 0.807399$$

$$f_o = \sqrt{f_1 f_2} = \sqrt{(30)(80)} = 48.989795 \text{ MHz}, \quad \omega_o = 2\pi f_o = 0.307812 \times 10^9$$

$$w = \frac{f_2 - f_1}{f_o} = \frac{80 - 30}{48.989795} = 1.020621$$

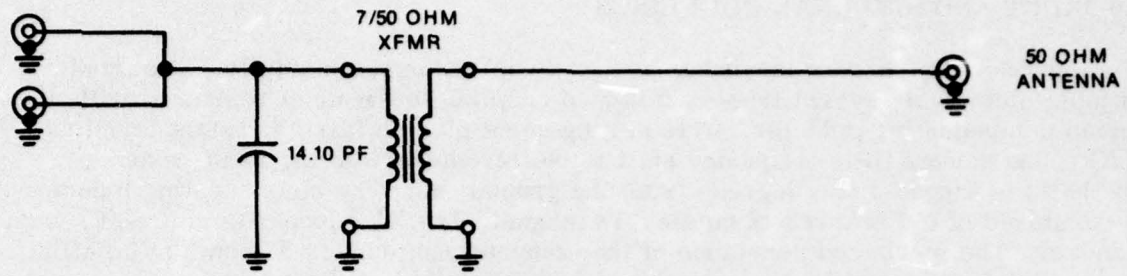
$$L_2 = \frac{g_2 R}{w \omega_o} = \frac{(0.947465)(50)}{(1.020621)(0.307812)} = 150.79 \text{ nH}, \quad C_2 = \frac{w}{\omega_o g_2 R} = \frac{(1000)(1.020621)}{(0.307812)(0.947465)(50)}$$

$$= 69.99 \text{ pF}$$

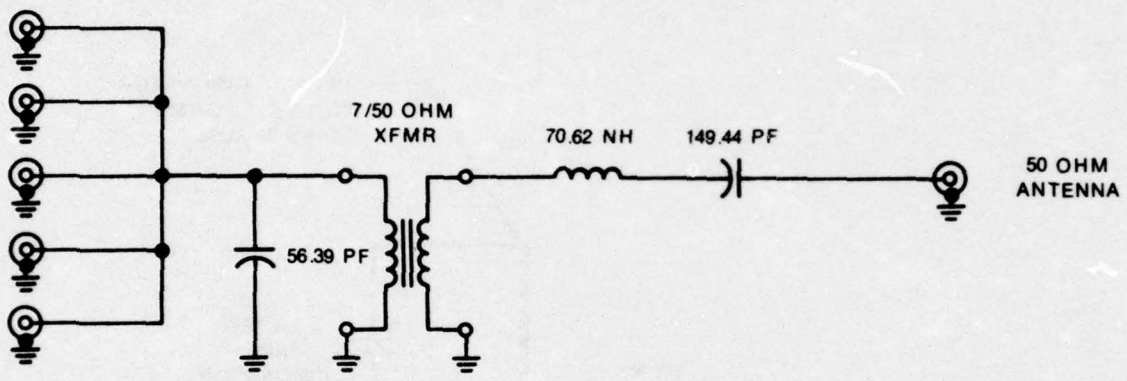
$$L_3 = \frac{w R}{\omega_o g_3} = \frac{(1.020621)(50)}{(0.307812)(0.892086)} = 185.84 \text{ nH}, \quad C_3 = \frac{g_3}{w \omega_o R} = \frac{(1000)(0.892086)}{(1.020621)(0.307812)(50)}$$

$$= 56.79 \text{ pF}$$

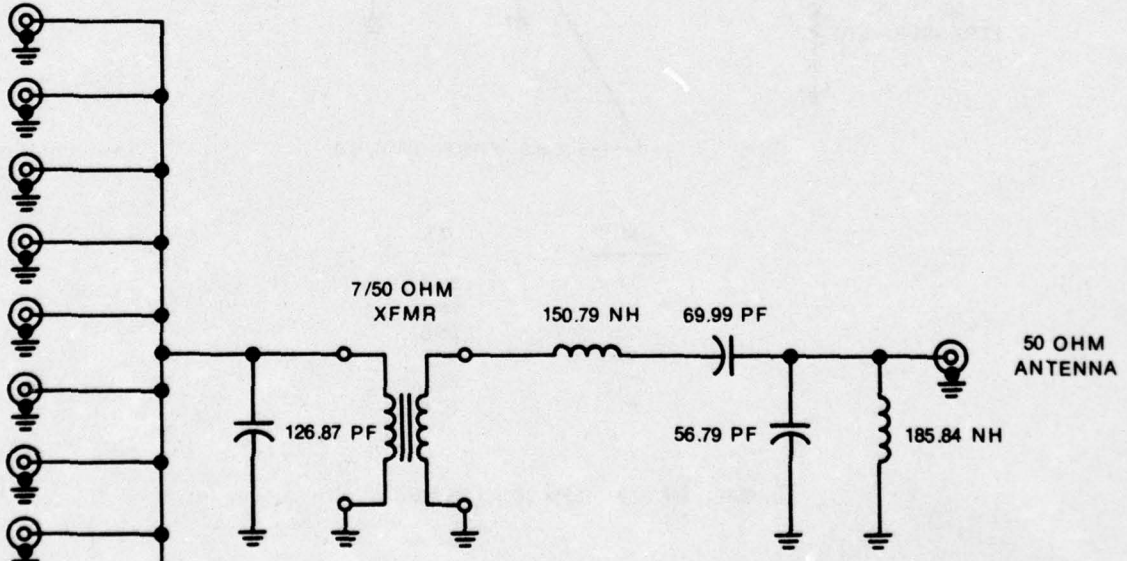
Figure 2.5-5. 10-Channel Multicoupler Matching Network Element Values.



2-CHANNEL MULTICOUPLER



5-CHANNEL MULTICOUPLER

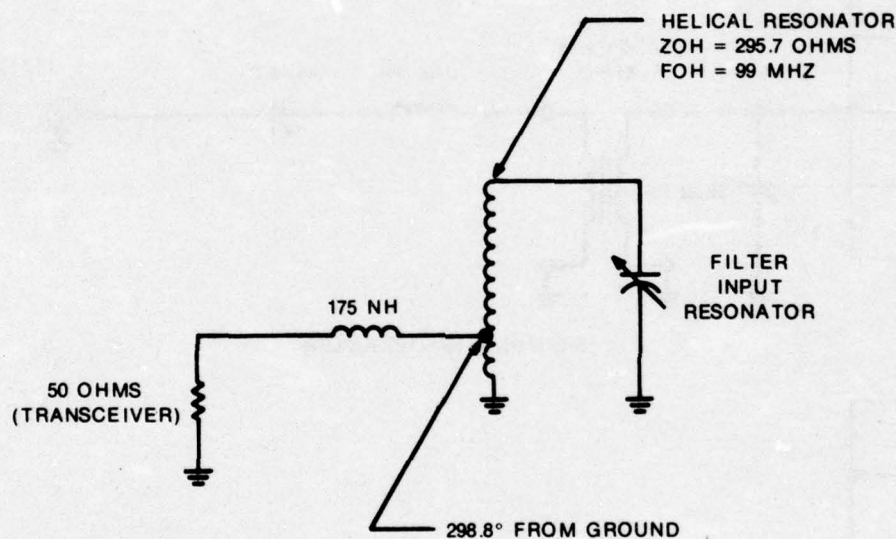


10-CHANNEL MULTICOUPLER

Figure 2.5-6. Final Multicoupler Configurations.

2.6 INPUT AND INTERNAL COUPLINGS

The input coupling arrangement has been determined experimentally. The most suitable method of several tried is a tapped coupling to the input resonator with a series compensating inductor. This arrangement gives a fairly constant terminal, Q (Q_t), and causes little frequency shift to be introduced into the input resonator. The helix is tapped 298.8 degrees from the ground end. The compensating inductor is composed of 6-1/2 turns of number 18 magnet wire, close wound, on a 15/64-inch mandrel. The measured reactance of the compensating coil is 33 ohms at 30 MHz. Figure 2.6-1 presents the measured terminal Q for this configuration.



F, MHZ	QT
30	59.4
40	56.4
50	56.6
60	57.5
70	59.2
80	60.6

DESIRED QT - 59, FROM 30 TO 80 MHZ

Figure 2.6-1. Measured Input Terminal Q .

Aperture coupling is used for the two internal couplings. This form of coupling can be made to agree very closely with the desired value. For a constant percentage bandwidth filter the coefficient of coupling should remain a constant value over the operating frequency range. In this case the magnitude of the coupling coefficient is 0.01695. Figure 2.6-2 presents the measured coupling for the depicted configuration.

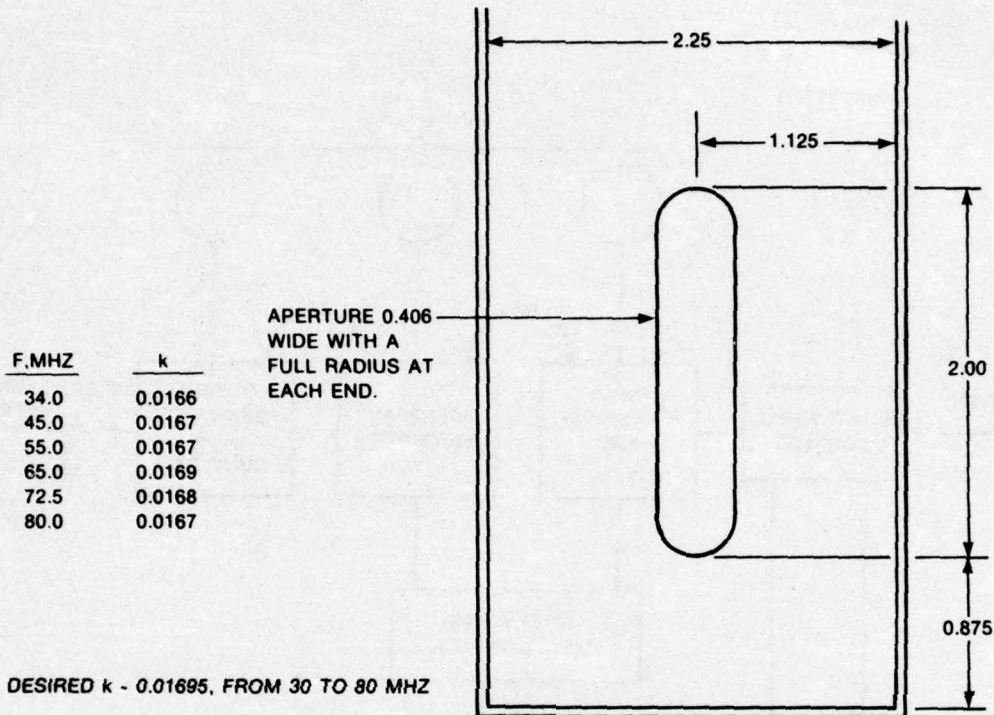


Figure 2.6-2. Measured Coupling Coefficient.

2.7 TUNING METHOD AND DISCRIMINATOR DESIGN

A block diagram of the filter is shown in figure 2.7-1. Two discriminators, a forward/reflected power discriminator (directional coupler), and a 90-degree phasing discriminator are employed to tune the filter. The use of two discriminators results in perfect tunes, that is, a symmetrical response shape.

The filter is basically tuned for minimum reflected power. The phasing function assures that the correct minimum reflected power point is used. The forward power indication is used as a monitoring function only.

Figure 2.7-2 shows a simplified schematic of the directional coupler. The reflected power detector operates in the following manner: a current sample is taken from the transmission line by means of a transformer. This provides a voltage across the load resistor proportional to the line current. This voltage is applied to the anode of the diode. Simultaneously a voltage sample is applied to the cathode end of the diode (derived from the capacitor divider). The transformer phasing and circuit constants are set up so that when the transmission line is terminated in its characteristic impedance (50 ohms) the two samples are equal in phase and magnitude; thus, the diode does not conduct and the reflected power output is zero. Any deviation of the terminating impedance from 50 ohms causes this balance to be upset. The diode then conducts proportional to the unbalance, giving a dc output voltage proportional to

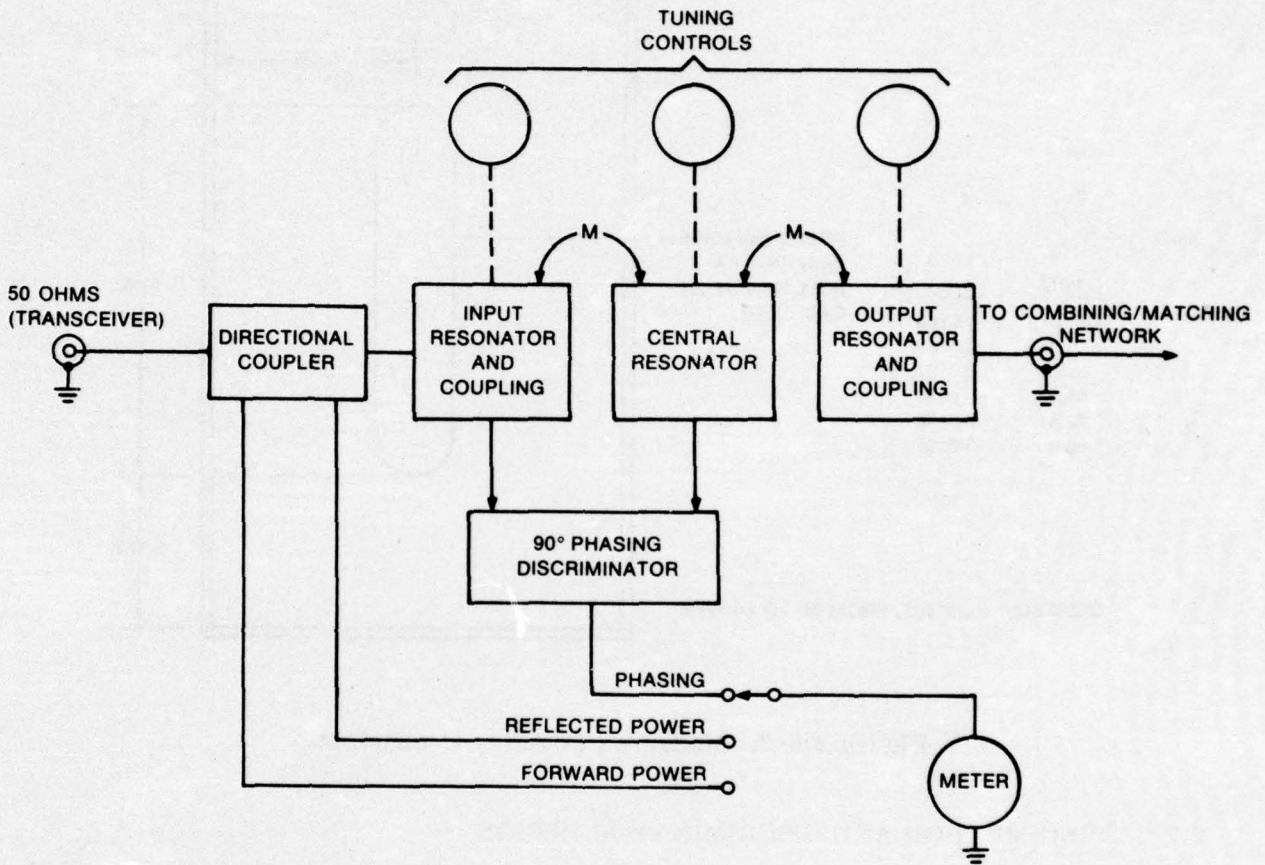


Figure 2.7-1. Filter, Simplified Block Diagram.

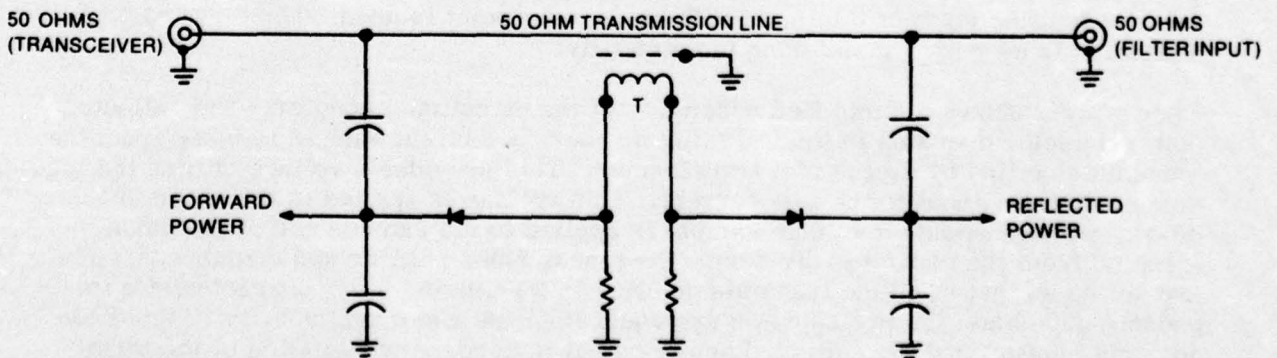


Figure 2.7-2. Simplified Directional Coupler Schematic.

reflected power. The forward power detector works in essentially the same manner except the current and voltage samples are 180 degrees out of phase. This results in the dc output voltage being a maximum when the transmission line is terminated in 50 ohms. Other values of terminating impedance cause the dc output voltage to vary proportional to the forward power.

Figure 2.7-3 shows a simplified schematic of the phasing discriminator. This is a conventional 90-degree discriminator. The voltage sample V_2 appears in the secondary of the transformer as two equal voltages but, 180 degrees different in phase with respect to the center tap. The second voltage sample V_1 is connected to the center tap. Thus, when V_1 and V_2 have a 90-degree relationship, the dc voltage appearing across the potentiometer is equal in magnitude and opposite in polarity with respect to the wiper of the potentiometer. The total voltage across the potentiometer is zero. As the phase relationship of the two voltages change the total voltage across the potentiometer is either positive or negative depending on whether V_1 leads or lags V_2 by more or less than 90 degrees. The magnitude depends on how greatly the angle between the two voltages differ. A bridge rectifier is connected to the output of the discriminator, this provides a unidirectional voltage output for the metering circuitry; for example, the output voltage of the bridge circuit is zero for a 90-degree phase relationship between V_1 and V_2 and positive going for any deviation from 90 degrees between the two voltage samples.

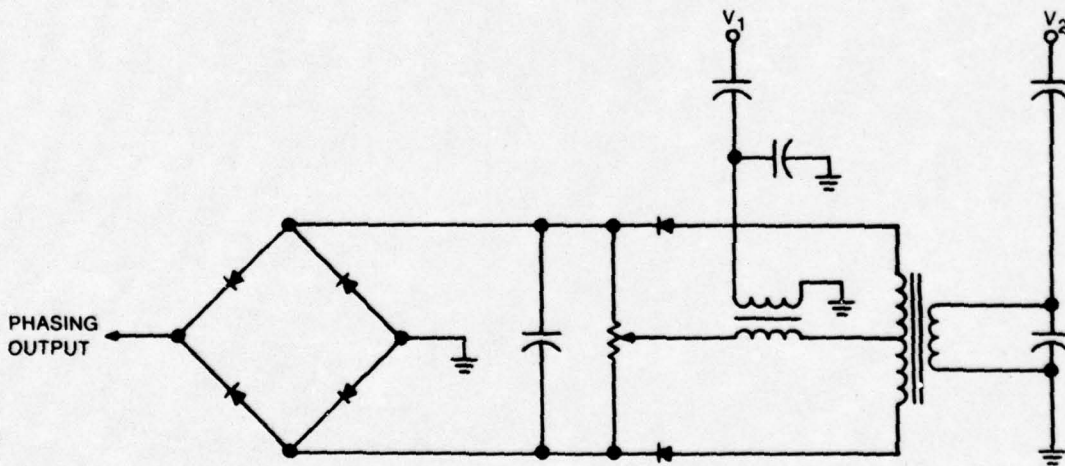


Figure 2.7-3. 90° Discriminator, Simplified Schematic.

Details of the 2- and 5-channel multicouplers in regard to physical configuration, electrical design, and measured performance are presented.

3.1 GENERAL DESCRIPTION

Figure 3.1-1 shows the 5-channel vhf transceiver multicoupler. Figure 3.1-2 depicts the 2-channel version. They consist of identical bandpass filter modules (shown in figure 3.1-3) and associated mounting bases. Collins commercial nomenclature has been assigned to the deliverable hardware. The filter has an 835P-1 type number. The 2-channel multicoupler is a 156W-1, and the 5-channel multicoupler a 156W-2. The mounting base in each case contains the matching and combining networks. An antenna connector (type N) is located on the right side of the mounting base in each case. Figure 3.1-4 shows the rear of the 5-channel multicoupler. The 5 transceiver connectors (type BNC) are located at the rear top edge of the bandpass filters. The 2-channel multicoupler is identical in appearance except for the number of bandpass filters.

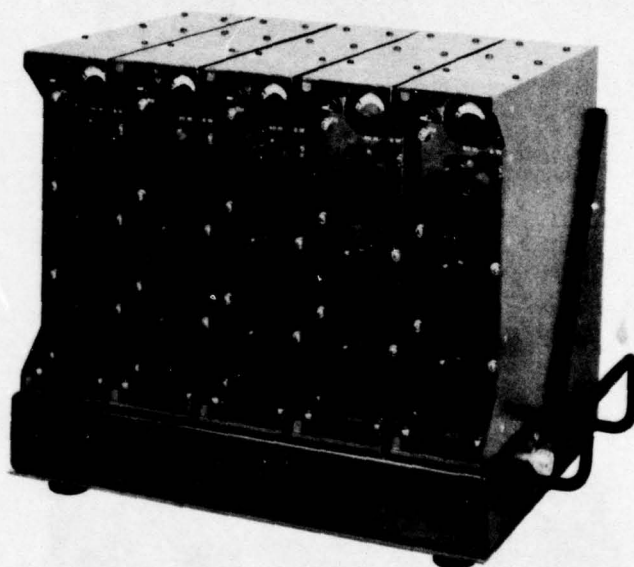


Figure 3.1-1. 5-Channel Multicoupler (156W-2).

Push-on rf connectors are used to connect the outputs of the bandpass filters to the matching networks located in the mounting bases. Figure 3.1-5 shows a 2-channel mounting base with the bandpass filters removed. The push-on rf connector may be seen at the rear top surface of the mounting base. The 5-channel version is identical in appearance except for the number of bandpass filters.

Four screws are used to retain each of the bandpass filters. Two are located on the lower front edge of the filter and two are located on the rear surface of the filter just below the transceiver connector. Controls and connectors are protected by panel extensions, and in the case of the output connector, by the carrying handle. Overall weight of the 2-channel multicoupler is 14.6 pounds, and 33.9 pounds for the 5-channel version.

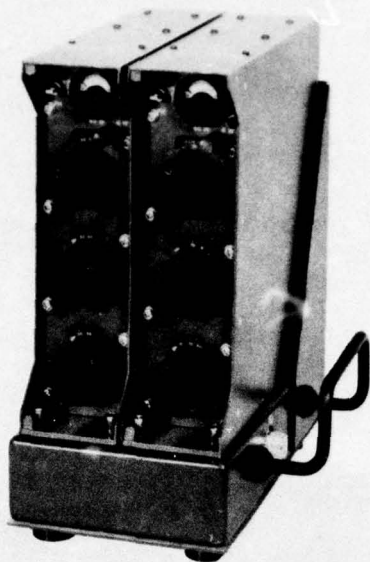


Figure 3.1-2. 2-Channel
Multicoupler
(156W-1).

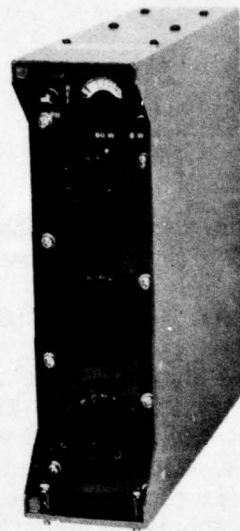


Figure 3.1-3. Bandpass
Filter
(835P-1).

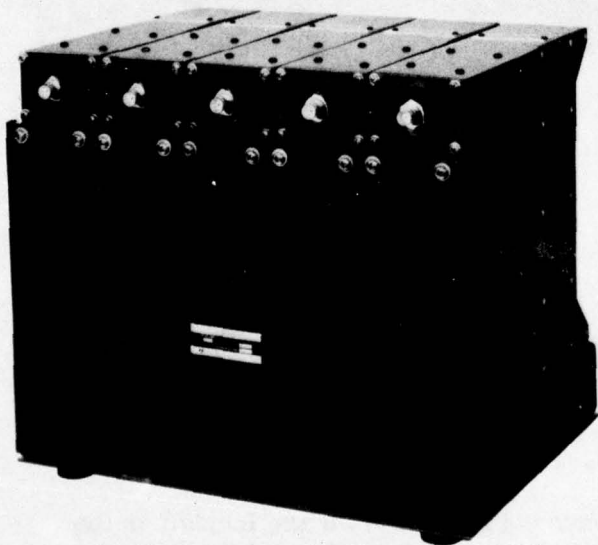


Figure 3.1-4. 5-Channel Multicoupler
(Rear View).

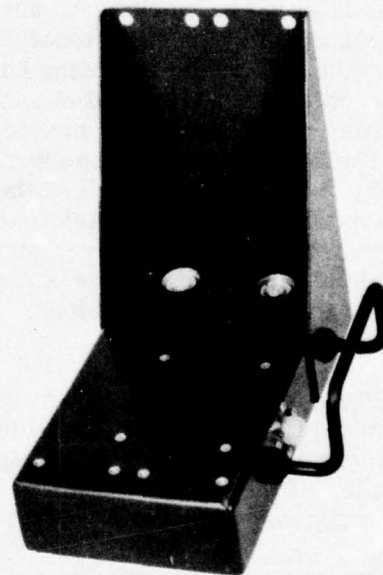


Figure 3.1-5. 2-Channel
Mounting
Base.

Each bandpass filter has 3 tuning knobs and frequency dials. The tuning knobs permit either course or fine adjustment, and each knob contains an integral knob lock. Tuning is accomplished by setting the three knobs to the desired frequency (indicated by the frequency dials), applying rf power, and adjusting for minimum reflected power and phasing error. The meter located on the top of the front surface is used to indicate forward power, reflected power, and phase error. A 3-position switch to the left of the meter allows selection of these functions. Immediately below the meter is a 2-position switch which allows the meter sensitivity to be changed; for example, 60 watts full scale, or 6 watts full scale.

Each version of the multicoupler has four feet located on the under surface of the mounting base. Each foot is attached with a single screw. The feet may be removed and the equipment permanently mounted using the same threaded mounting holes. Any filter may be removed without disturbing the remaining filters. This can also be accomplished with the multicoupler permanently mounted.

3.2 MEASURED PERFORMANCE

The measured performance is a summary of data taken on the 2-channel and 5-channel multicouplers.

Figure 3.2-1 shows the minimum/maximum insertion loss from measuring the 7 communication channels of the two multicouplers at room temperature. As can be seen the insertion loss lays between 1.66 and 1.22 dB.

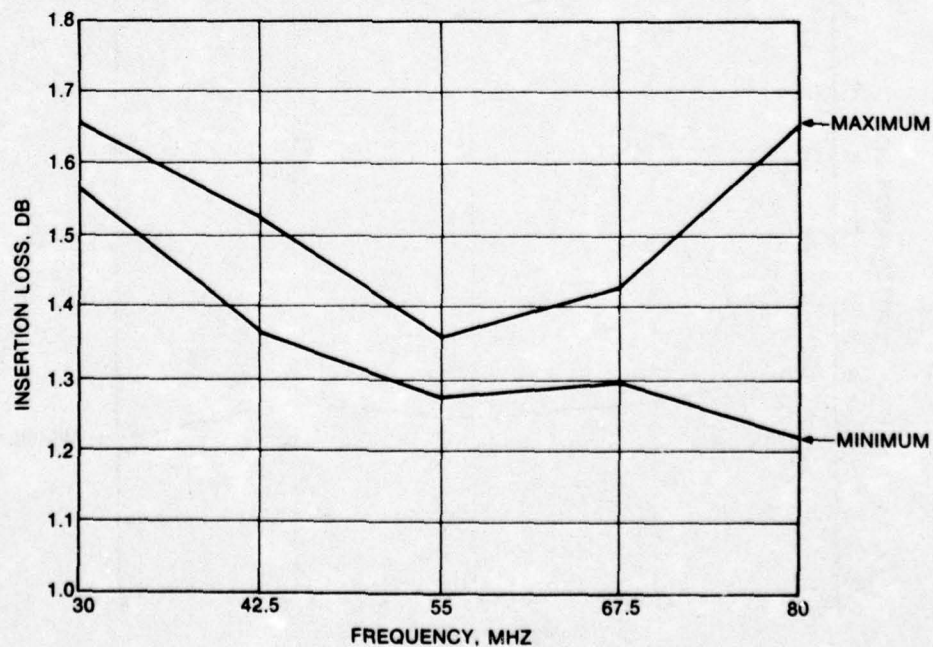


Figure 3.2-1. Measured Insertion Loss.

The measured transceiver port to antenna port attenuation is shown in figure 3.2-2. The minimum/maximum contours are the result of measuring the seven communication channels. The value of attenuation obtained is at both the upper and lower 5-percent frequency spacing. The minimum attenuation obtained was 39.2 dB.

Table 3.2-1 presents a summary of the other performance parameters that were measured. Input vswr was less than 1.33:1 in all cases. Intermodulation distortion varied between 126 and 143 dB below 60 watts. For this case two 60-watt power sources were used at a frequency separation of 5 percent. Transceiver port to transceiver port attenuation was found to be greater than 51.9 dB for channel spacings of 5 percent. Harmonic generation varied between 129 and 158 dB. Measurements were made at the 2nd, 3rd, 4th, and 5th harmonic.

All of the above room temperature data is within the specification limits except for intermodulation distortion (IMD). It is felt that the IMD performance is about the limit of what can be achieved for a tunable design having removable filter modules. The IMD level is very low and is due to several metal-to-metal connections that cannot be soldered due to other considerations. These connections are associated with the variable tuning capacitor (internal contact fingers and external bushing mount) and the connector interface between the filters and the mounting base.

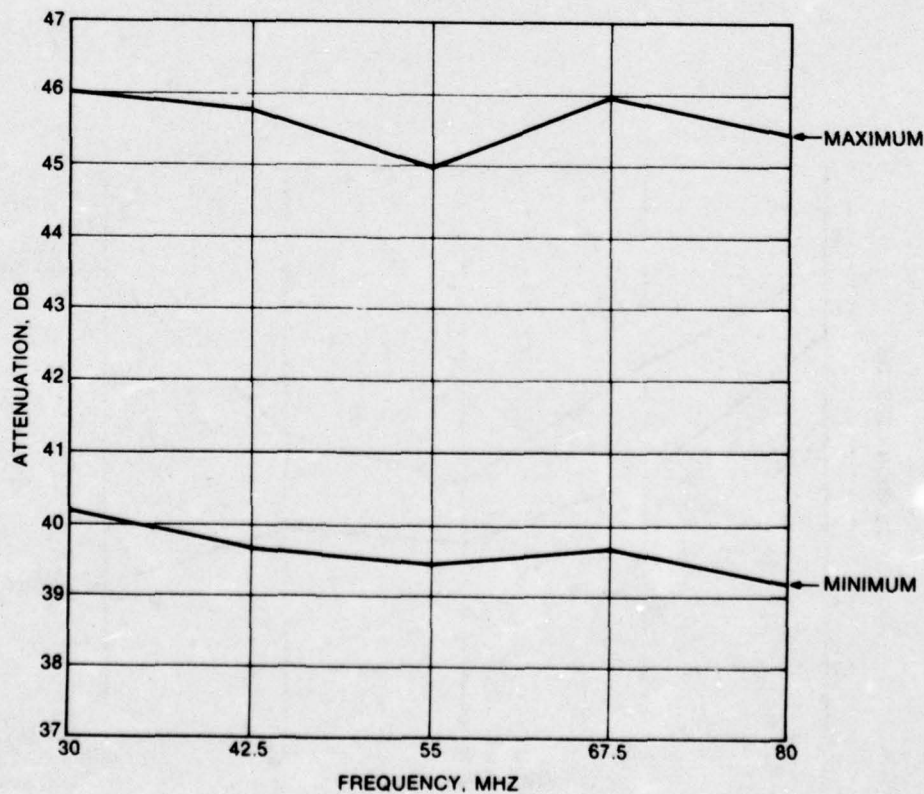


Figure 3.2-2. Measured Transceiver to Antenna Port Attenuation.

Table 3.2-1. Measured Performance Data.

MEASURED QUANTITY	MINIMUM	MAXIMUM
Vswr	1.03:1	1.33:1
Intermodulation distortion	126 dB below 60 watts	143 dB below 60 watts
Transceiver to transceiver attenuation	51.9 dB	54.8 dB
Harmonic generation	129 dB below 60 watts	>158 dB below 60 watts

A series of environmental tests were performed on the 2-channel and 5-channel multicoupler. The tests performed were: high temperature, low temperature, rain, humidity, altitude, dust, vibration, shock, and bench handling. The results of these tests (procedures, measured data, discussion of results, and recommendations) are presented in the Contractor's Evaluation Report, dated 21 June 1976. In general, however, the equipment performed well except in two areas. One, a problem was discovered during low temperature testing. It was traced to the fact that the variable tuning capacitors had inadvertently been pressurized with the wrong gas mixture. An additive to prevent the gas from liquefying at low temperature was omitted. This omission caused changes in dielectric constant and capacitor push force below 0 °C. Two, a problem with stiffness of the bottom plates on the multicoupler mounting bases was uncovered during vibration. This resulted in high g forces being applied to the filter modules. Even under these conditions the equipment performed fairly well; six of the seven communication channels remained within the specified performance limit. The one channel's insertion loss exceeded the limit after the vibration test was completed. Both of these problem areas are minor in nature and can be remedied easily on future equipments.

3.3 PHYSICAL CONFIGURATION

An exploded view of the bandpass filter module is shown in figure 3.3-1. The filter case is constructed of silver plated aluminum. Gear plates, rear cover, and front panel are also aluminum. The front panel contains the metering circuitry, tuning knobs, and frequency dials. The front panel/gear assembly easily separates from the remainder of the filter as shown in the figure. Separation takes place at the three capacitor spline drives. The circuit card assembly visible in the figure is the 90-degree discriminator. Immediately to the right of the 90-degree discriminator card is a 3-terminal feedthrough bushing, which brings the dc signal from the directional coupler up to the front panel area.

Figure 3.3-2 shows the rear of the filter with the rear cover removed. The output connector and resonator are on the top. Ground connections of the helix are clearly visible. The input coupling inductor, L7, is visible in the lower resonator compartment (input resonator). At the bottom is the directional coupler printed circuit board and transceiver connector. Additional details of the capacitor drive assembly are shown in figures 3.3-3 and 3.3-4. Figure 3.3-5 shows a complete filter with the side access cover removed, and figure 3.3-6 shows a good view of the transceiver connector and interface connector.

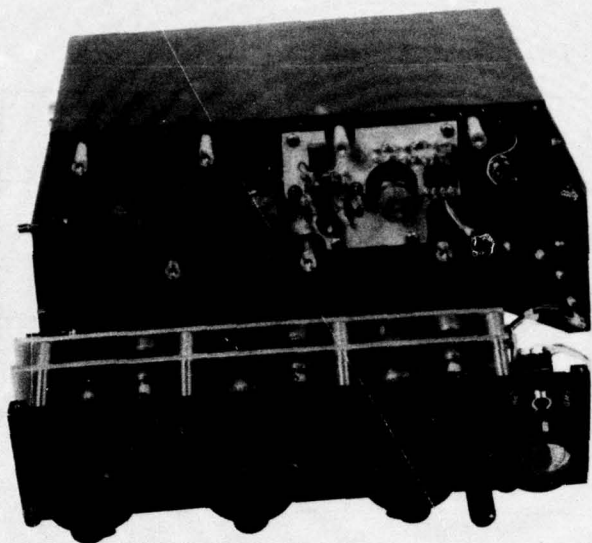


Figure 3.3-1. Bandpass Filter, Exploded View.

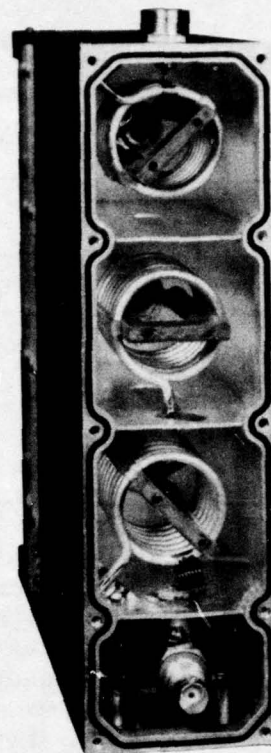


Figure 3.3-2. Helical Resonator Detail.

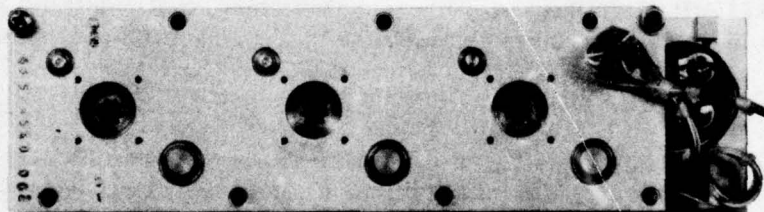


Figure 3.3-3. Drive Assembly, Rear View.

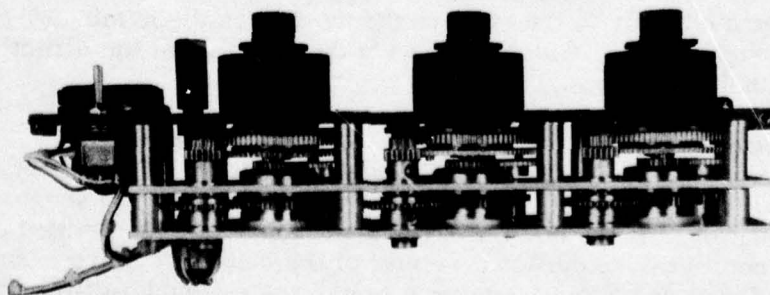


Figure 3.3-4. Drive Assembly, Side View.

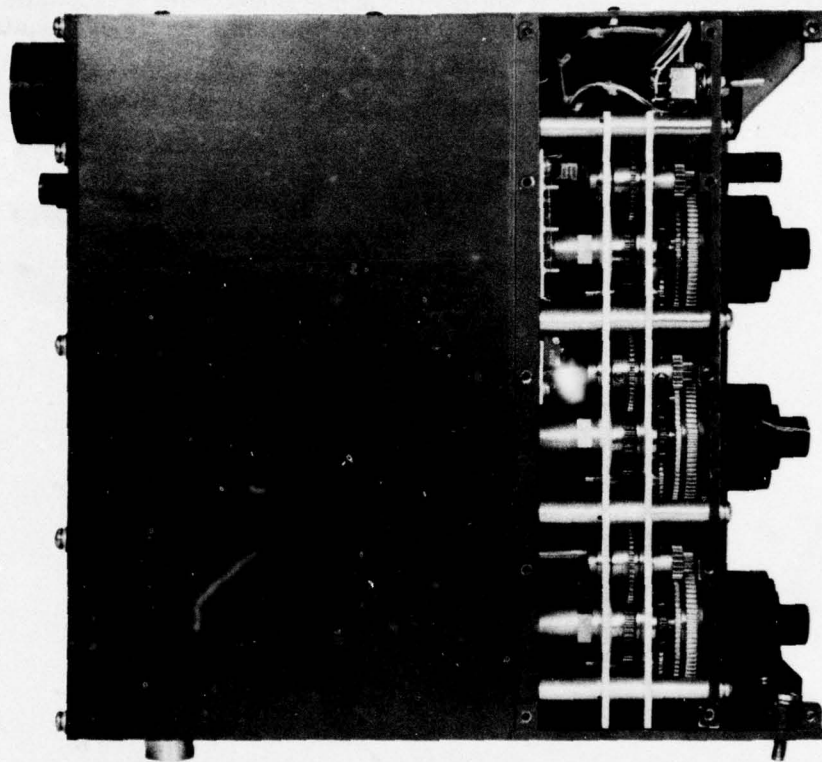


Figure 3.3-5. Filter Side View, Access Cover Removed.

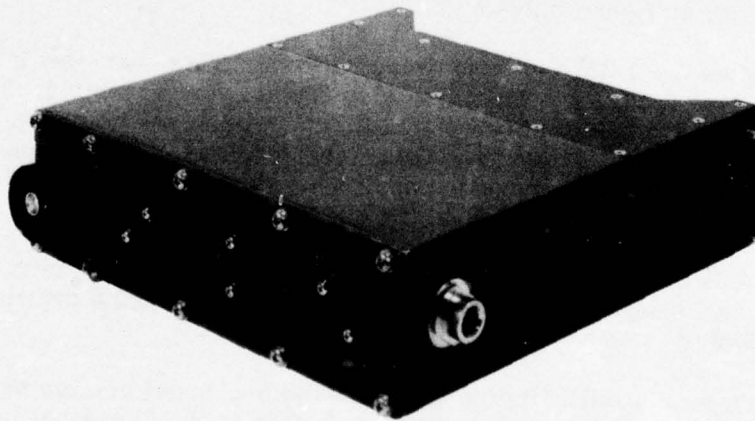


Figure 3.3-6. Bandpass Filter, RF Connector Locations.

The directional coupler printed circuit board assembly is shown in figure 3.3-7. The coupling transformer is mounted in the center of the board with the coaxial cable leaving the board on the left and right sides. All other components are lead mounted with the exception of the two air variable trimmer capacitors, C3 and C7.

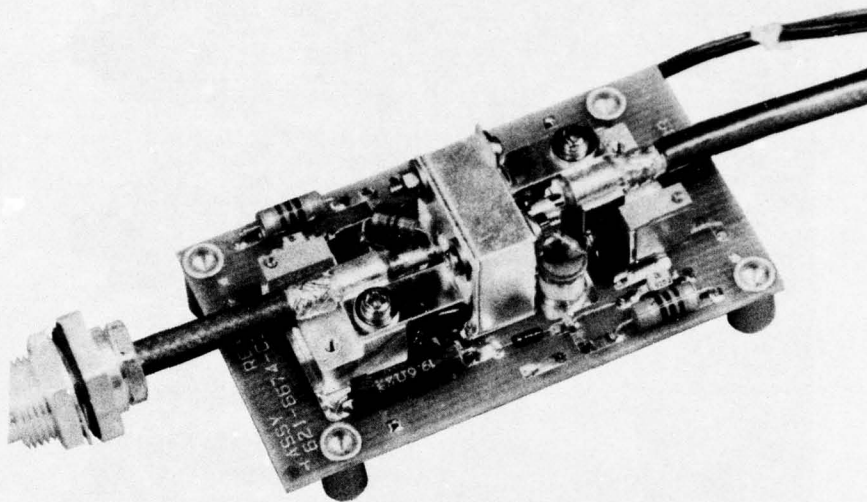


Figure 3.3-7. Directional Coupler Assembly.

Maximum overall dimensions of the bandpass filter are: 2.38 inches wide, 8.62 inches high, and 8.88 inches deep. The weight is 5.4 pounds. An outline drawing of the bandpass filter is shown in figure 3.3-8.

Figure 3.3-9 shows the 2-channel combining network. This is a view into the interior of the mounting base from the bottom, prior to foaming the assembly. The transformer assembly is at the left of the figure. Note all connections are soldered to reduce IMD to the lowest possible level. The metal jacketed coaxial interconnect lines have sleeving installed over the outer conductors. This is to prevent possible pressure contacts from occurring during the foaming operation.

Overall dimensions of the 2-channel multicoupler are: 5.4 inches wide, 11.2 inches high, and 9.6 inches deep. The weight is 14.6 pounds. An outline drawing of the 2-channel multicoupler is shown in figure 3.3-10.

Figure 3.3-11 shows a similar interior view of the 5-channel combining network and mounting base. Note that the construction is similar to the 2-channel unit except that 5 interconnecting coaxial lines are used. Also, the series reactance compensation network can be seen installed between the transformer assembly and the antenna connector. This compensation network is not required in the 2-channel version as discussed in section 2.5.

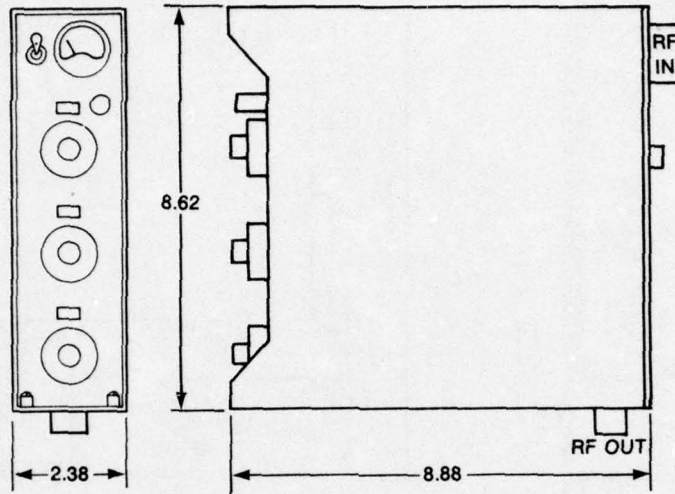


Figure 3.3-8. Outline Drawing, Bandpass Filters.

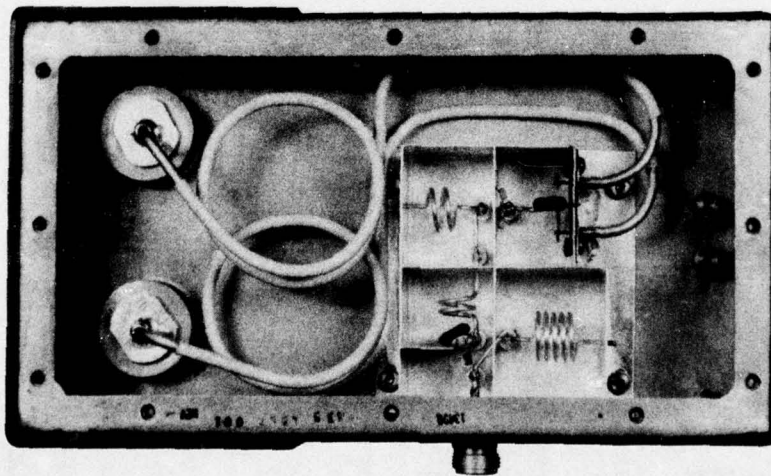


Figure 3.3-9. 2-Channel Network and Mounting Base.

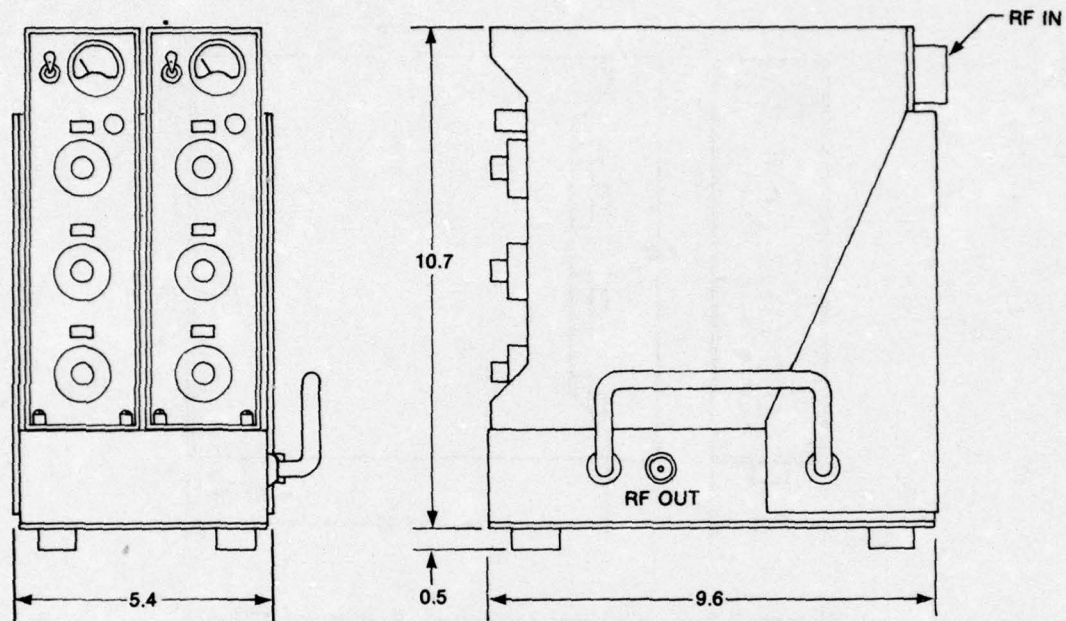


Figure 3.3-10. Outline Drawing, 2-Channel Multicoupler.

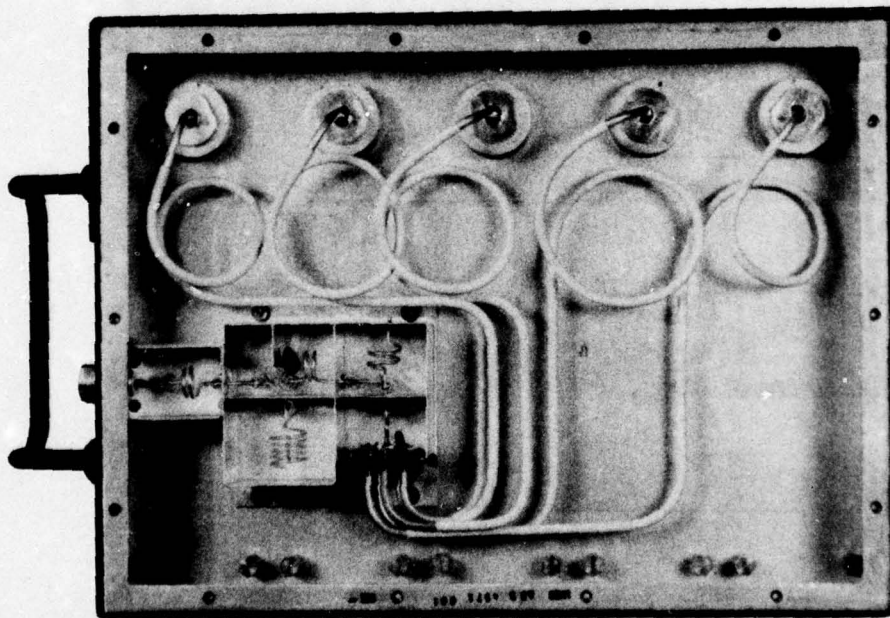


Figure 3.3-11. 5-Channel Network and Mounting Base.

Overall dimensions of the 5-channel multicoupler are: 12.9 inches wide, 11.2 inches high, and 9.6 inches deep. The weight is 33.9 pounds. An outline drawing of the 5-channel multicoupler is shown in figure 3.3-12.

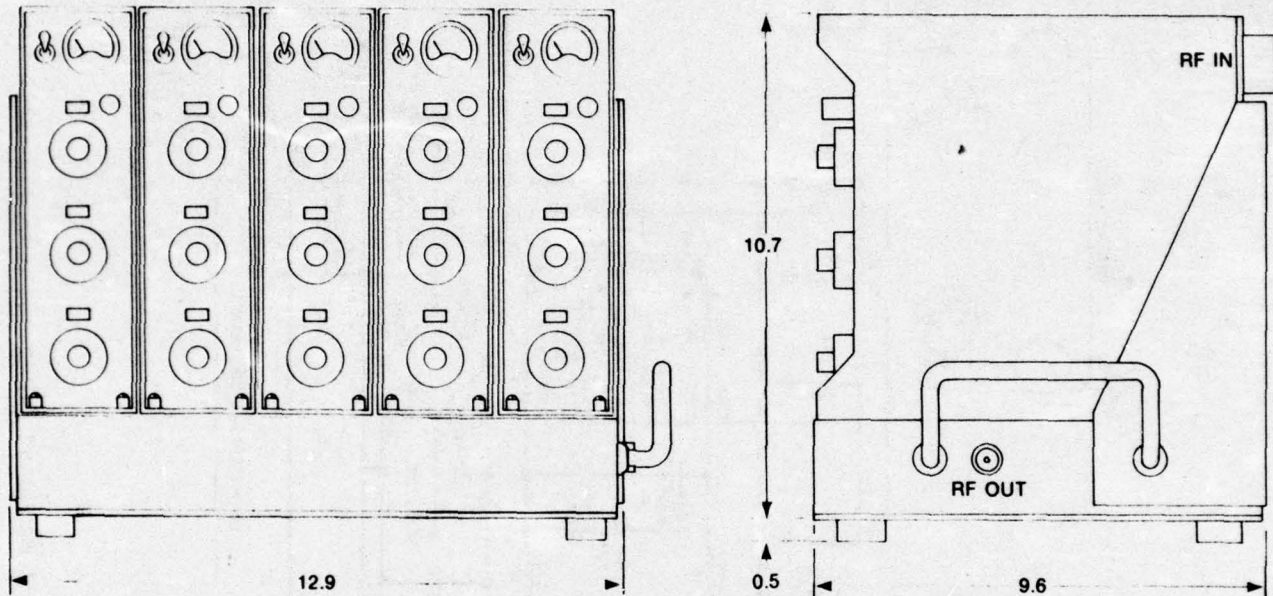


Figure 3.3-12. Outline Drawing, 5-Channel Multicoupler.

3.4 SCHEMATICS, PARTS LISTS, AND TUNING PROCEDURE

A schematic of the 835P-1 Bandpass Filter is shown in figure 3.4-1. Table 3.4-1 gives a list of electrical parts used in the filter.

Schematics of the 2-channel and 5-channel combining networks are shown in figures 3.4-2 and 3.4-3. Electrical parts lists for these two units are shown in table 3.4-2 (156W-1, 2-channel multicoupler) and table 3.4-3 (156W-2, 5-channel multicoupler).

Table 3.4-4 gives a step-by-step tuning procedure for the 2- and 5-channel multicouplers. This is identical to the procedure supplied with the deliverable hardware.

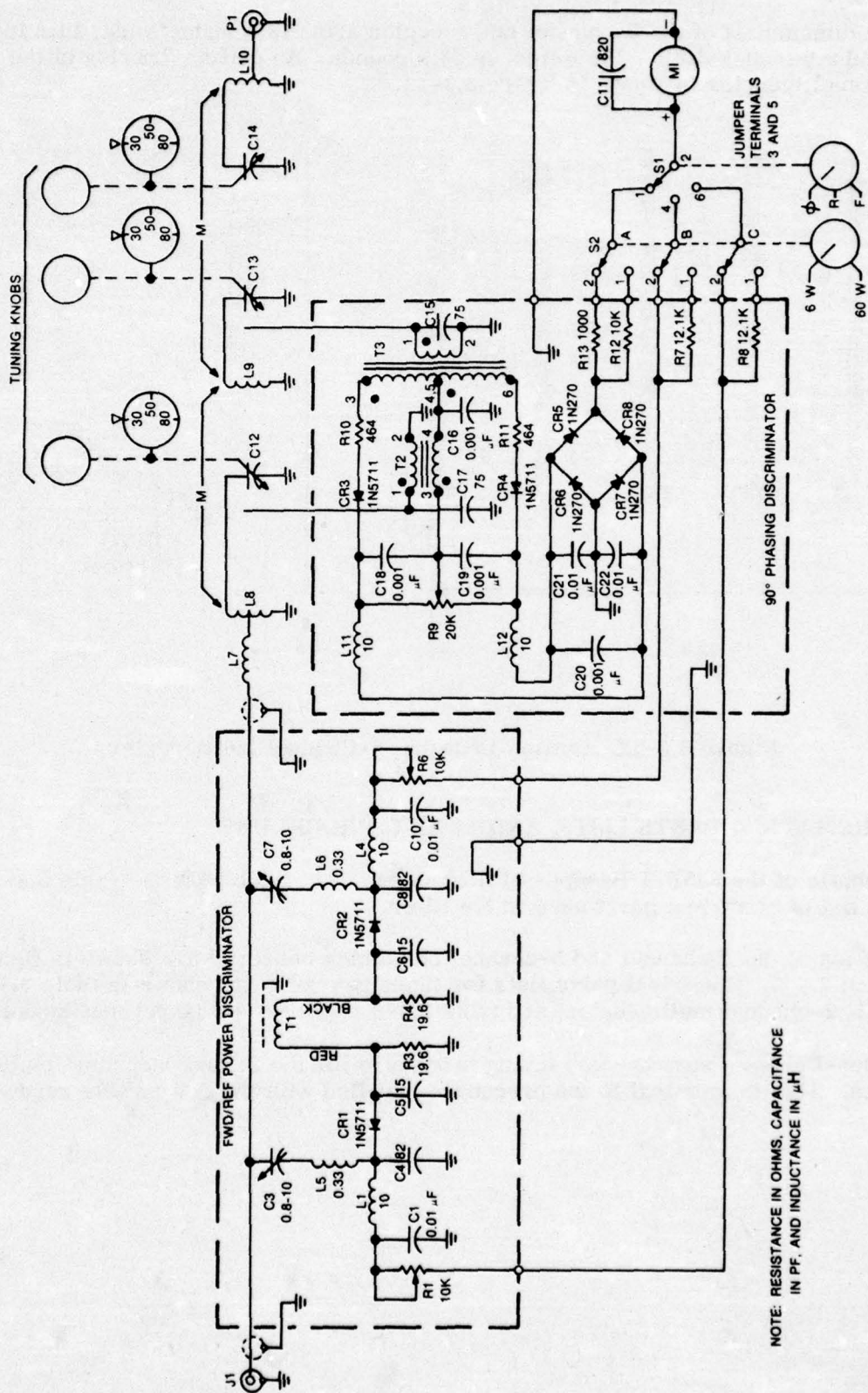


Figure 3.4-1. Schematic, 835P-1 Bandpass Filter.

Table 3.4-1. VHF Filter 835P-1, Parts List.

SYMBOL NO	QUANTITY PER ASSY	COLLINS PART NUMBER	DESCRIPTION	MIL TYPE
C1, C10, C21, C22	4	913-9011-180	0.01 μ F ceramic capacitor	CKR05
C3, C7	2	922-0595-010	0.8- 10-pF var capacitor	Per MIL-C-14409
C4, C8	2	914-3078-000	82 pF ceramic capacitor	None
C5, C6	2	912-2095-080	15-pF mica capacitor	Per MIL-C-39001/5
C11	1	913-1190-000	820-pF ceramic capacitor	CX60
C12, C13, C14	3	919-0287-010	1.5- 45-pF var capacitor	None
C15, C17	2	912-4141-340	75-pF mica capacitor	None
C16, C18, C19, C20	4	913-9008-380	0.001 μ F ceramic capacitor	CKR05
CR1, CR2, CR3, CR4	4	353-9008-180	1N5711 diode	JAN 1N5711
CR5, CR6, CR7, CR8	4	353-2016-000	1N270 diode	JAN 1N270
L1, L4	2	240-1580-000	10- μ H rf choke	MS-14046/4
L5, L6	2	240-2017-000	0.33- μ H rf choke	MS-75083-07
L11, L12	2	240-2035-000	10- μ H rf choke	MS-75084-12
J1	1	357-9248-010	BNC connector	UG-909B/U
M1	1	476-0219-040	Meter, 200 μ A fs	Per MIL-M-17275 except for scale
R1, R6	2	381-1853-200	10K potentiometer	Per MIL-R-27208

Table 3.4-1. VHF Filter 835P-1, Parts List (Cont).

SYMBOL NO	QUANTITY PER ASSY	COLLINS PART NUMBER	DESCRIPTION	MIL TYPE
R3, R4	2	714-0011-010	19.6-ohm resistor	RD60P119RG6
R7, R8	2	724-0639-990	12.1K-ohm resistor	RNC55K
R9	1	380-4041-000	20K potentiometer	None
R10, R11	2	724-0638-620	464-ohm resistor	RNC55K
R12	1	724-0639-910	10K-ohm resistor	RNC55K
R13	1	724-0638-940	1000-ohm resistor	RNC55K
S1	1	266-5321-650	1P3T toggle switch	None
S2	1	259-9487-070	3 pole, 2 pos, rotary switch	None
Part of T1	1	288-2476-000	Transformer core	None
Part of T2, T3	2	288-0778-000	Transformer core	None
--	2 ft.	425-1106-010	50-ohm coaxial cable	None

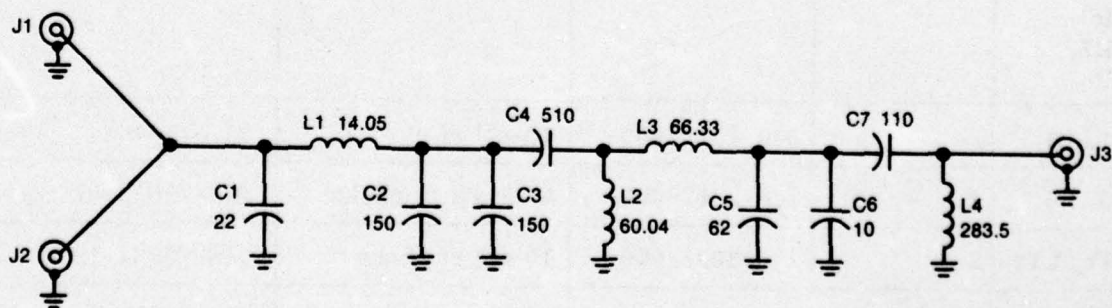


Figure 3.4-2. Schematic, 2-Channel Combining Network.

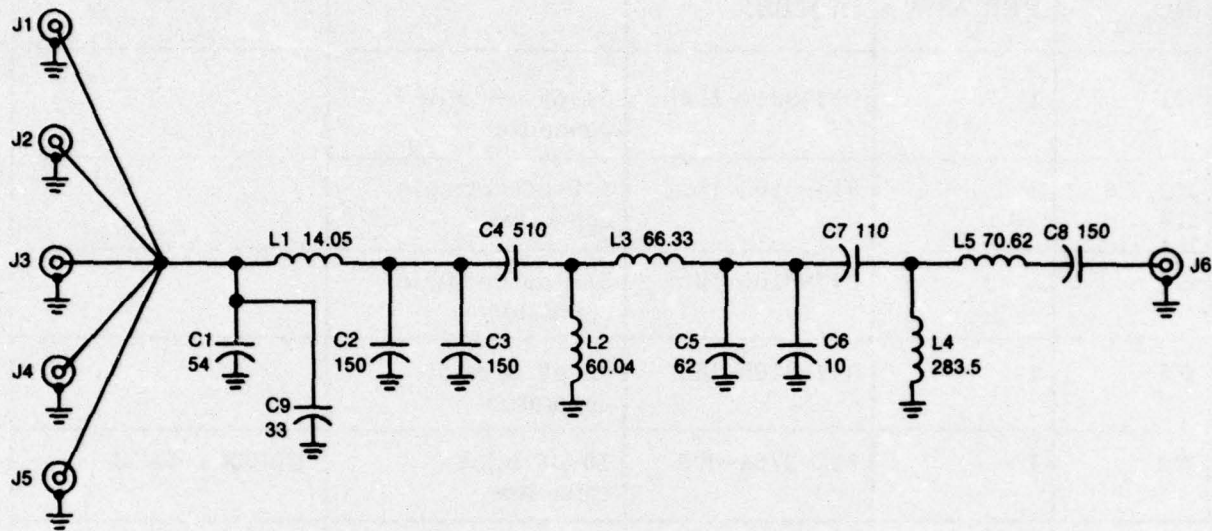


Figure 3.4-3. Schematic, 5-Channel Combining Network.

Table 3.4-2. 156W-1 Parts List, 2-Channel Multicoupler.

SYMBOL NO.	QUANTITY PER ASSY	COLLINS PART NUMBER	DESCRIPTION	MIL TYPE
C1	1	912-2768-000	22-pF mica capacitor	CM05E2205J03
C2, C3	2	914-3105-180	150-pF ceramic capacitor	
C4	1	914-3105-190	510-pF ceramic capacitor	
C5	1	914-3105-160	62-pF ceramic capacitor	
C6	1	912-2754-000	10-pF mica capacitor	CM05C100K03
C7	1	914-3105-170	110-pF ceramic capacitor	
J3	1	357-9003-000	Type N connector	UG-58A/U
	4 ft	425-1630-000	50-ohm metal jacket coax	UG-402/U

Table 3.4-3. 156W-2 Parts List, 5-Channel Multicoupler.

SYMBOL NO.	QUANTITY PER ASSY	COLLINS PART NUMBER	DESCRIPTION	MIL TYPE
C1	1	914-3244-110	54-pF ceramic capacitor	
C2, C3, C8	3	914-3105-180	150-pF ceramic capacitor	
C4	1	914-3105-190	510-pF ceramic capacitor	
C5	1	914-3105-160	62-pF ceramic capacitor	
C6	1	912-2754-000	10-pF mica capacitor	CM05C100K03
C7	1	914-3105-170	110-pF ceramic capacitor	
C9	1	912-2780-000	33-pF mica capacitor	CM05E330J03
J6	1	357-9003-000	Type N connector	UG-58A/U
	10 ft	425-1630-000	50-ohm metal jacket coax	UG-402/U

Table 3.4-4. Tuning Procedure for the 156W-1/156W-2 Multicoupler.

I. Prior to Tuning, Check the Following Conditions:

1. No other filters are tuned to, or within 5%, of the frequency about to be used.
2. Rf power input to the filter will not exceed 60 watts.
3. The output port of the multicoupler is terminated with a 50-ohm load or equivalent.

II. Initial Adjustments Before Applying RF Power:

1. Disengage the lock on the three tuning controls with a CCW rotation of the lock knobs.
2. Using the three large tuning knobs set the desired frequency in the center of the dial windows.
3. Set the meter function switch to the reflected power (REF) position.
4. Set the level switch to the 60-watt full scale (60 W) position.

III. Tuning Adjustments With RF Power Applied:

1. Apply rf power.
2. Starting with the top fine tune knob, adjust for minimum (REF) power. Proceed to the center and bottom fine tune knobs, adjusting each for minimum (REF) power.
3. Depress and hold the function switch in the (PH) position. Adjust the center fine tune knob for zero (PH) error. Note: Zero (PH) error will be indicated by a zero reading on the meter with a very sharp up-scale deflection on either side of the tune point.
4. Released the function switch to the (REF) position. Readjust the top and bottom fine tuning knobs for minimum (REF) power.
5. Recheck for zero (PH) error, with the function switch in the (PH) position, using the center fine tune knob.
6. Repeat steps 4 and 5 until lowest (REF) power and zero (PH) error is attained. Tuning is now complete.

IV. Additional Notes:

1. A more accurate tune may be achieved after completing section III, step 5, by setting the level switch to the 6-watt (6 W) position. This provides increased sensitivity of the (REF) power and (PH) error indications.
2. Forward power level can be measured at any time by placing the function switch in the (FWD) position. Full scale power readings of 6 watts (6 W) or 60 watts (60 W) are selected using the level switch.
3. To prevent possible damage, rf power should not be applied before section II is completed. Rf power should not be applied for a prolonged period (in excess of 1 minute) until section III has been completed.

Alternate Design Approach (2-Pole Filter)

In this section a simplified version of the transceiver multicoupler is explored. The basic change is to use a 2-pole filter design instead of a 3-pole filter design. This change however results in other simplifications as discussed below, and also results in some performance trade-offs.

4.1 GENERAL DESIGN CONSIDERATIONS.

The following assumptions are made regarding the alternate design:

- a. It will provide a minimum of 40-dB isolation from transceiver port to transceiver port.
- b. The filter design will incorporate 2 poles.
- c. The existing gas-filled variable tuning capacitor will be used.
- d. Resonator size will be the same as for the 3-pole design.
- e. The same matching/combining network philosophy as used on the deliverable hardware will be retained.
- f. The maximum rf power input to each channel will be 60 watts.

The retention of the gas-filled variable tuning capacitor is important, due to the time and expense of developing a unit of this type. With this constraint, it is necessary to preserve approximately the same peak resonator voltage as in the 3-pole version. This is synonymous to maintaining the same terminal Q, since:

$$E_p = \sqrt{2P Q_t X_{Le}}$$

The power (P) remains at 60 watts, X_{Le} is bounded by the output coupling requirements as discussed in paragraphs 2.3 and 2.4. Thus, approximately the same terminal Q is required to limit the peak resonator voltage to its present value.

It appears that the transceiver port to transceiver port attenuation is about 10 dB greater than the filter selectivity (L_S). This may be seen by comparing the transceiver port to transceiver port attenuation with the transceiver port to antenna port attenuation (paragraph 3.2). This added attenuation is due to using transmission line couplings between the filters output resonators and the common junction.

Thus, the design values of L_S should be something in excess of 30 dB, to preserve a 40-dB specification for the transceiver port to transceiver port attenuation. To assure specified performance into vswr loads, L_S should be 36 dB minimum.

From paragraph 2.2, for $n = 2$:

$$L_S = 10 \log \frac{1}{4} [b^4 + 4] \text{ where: } b = 2Q_{tu}$$

Letting $u = 0.1$, and $Q_t = 59$, gives:

$$b = 2Q_{tu} = (2)(59)(0.1) = 11.8$$

And:

$$L_S = 10 \log \frac{1}{4} [b^4 + 4] = 36.856 \text{ dB}$$

A 10-percent frequency spacing is required for the same selectivity as the 3-pole filter with a 5-percent frequency spacing.

The insertion loss of the 2-pole design will be less by the amount calculated below. Using $Q_t = 59$ and the measured unloaded Q (Q_u) at 30 MHz from table 2.2-1 in the insertion loss expression from paragraph 2.2, the insertion loss is:

$$\underline{n = 2}$$

$$L_o = 10n \log \left(1 + \frac{Q_t}{Q_u} \right) = 20 \log \left(1 + \frac{59}{671.3} \right) = 0.732 \text{ dB}$$

$$\underline{n = 3}$$

$$L_o = 10n \log \left(1 + \frac{Q_t}{Q_u} \right) = 30 \log \left(1 + \frac{59}{671.3} \right) = 1.098 \text{ dB}$$

$$L_o = 1.098 - 0.732 = 0.366$$

The insertion loss specification for the various multicoupler configurations may be lowered by 0.35 dB, or:

2-channel multicoupler, $L_o = 1.4 \text{ dB}$

5-channel multicoupler, $L_o = 1.65 \text{ dB}$

10-channel multicoupler, $L_o = 2.15 \text{ dB}$

Eliminating one resonator from the filter also allows exact tuning of the filter without the use of the 90-degree discriminator. Tuning can now be performed using only the reflected power function. Additional cost savings may be effected by using a single speed tuning knob on each capacitor drive. This would require slightly more effort to tune the filter since the operator would not have the high speed slew function available.

In addition to a cost advantage for the single speed drive, a knob lock function could be provided which would lock both knobs with a single locking control. Also a more positive lock could be achieved as compared to the present design.

Figure 4.1-1 shows the outline dimensions of the 2-pole filter. The filter has the same width and depth as the present design. The height has been reduced by 2.25 inches.

Figure 4.1-2 shows the outline dimensions of a 2-channel multicoupler. Again the width and depth remain the same but the height is 2.25 inches less.

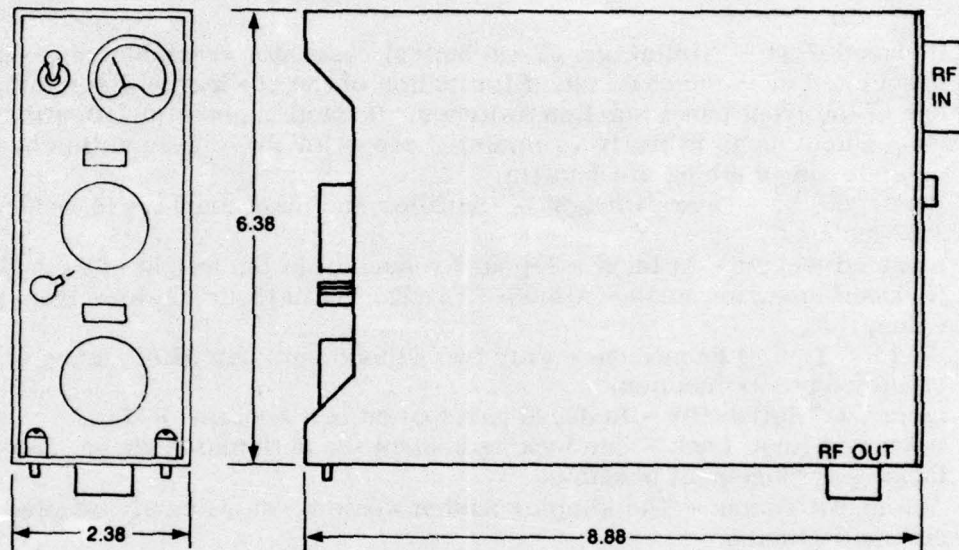


Figure 4.1-1. Outline Drawing, 2-Pole Bandpass Filter.

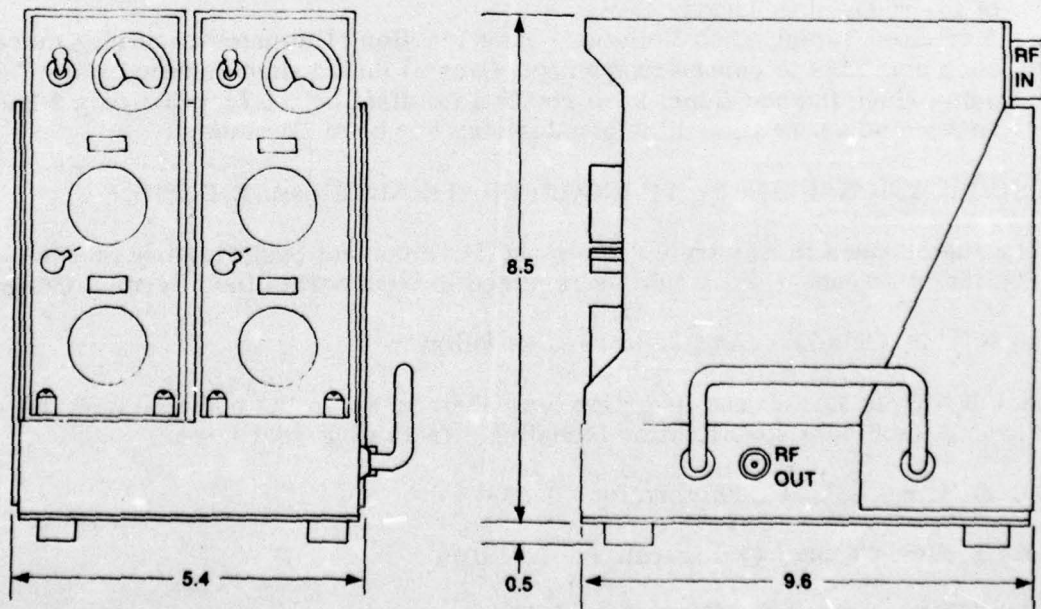


Figure 4.1-2. Outline Drawing, 2-Channel Multicoupler (Alternate Design).

4.2 ADVANTAGES AND DISADVANTAGES

The following lists the advantages and disadvantages of the 2-pole design as compared to the present 3-pole design.

a. Advantages

1. **Reduced Cost** - Elimination of one helical resonator, variable capacitor, and associated drive mechanism. Elimination of the 90-degree discriminator and one of the front panel function switches. Reduction and simplification of mechanical parts in the two remaining capacitor drive assemblies by using a single speed tuning mechanism.
2. **Reduced Size** - Overall height of the filter and multicouplers is reduced by 2.25 inches.
3. **Reduced Weight** - At least a 1-pound reduction in the weight of each filter.
4. **Reduced Insertion Loss** - A 0.35-dB reduction in insertion loss from present value.
5. **Simpler Tuning Procedure** - Only two adjustments per filter, using only the reflected power function.
6. **Increased Reliability** - Reduced parts count and simpler design.
7. **Improved Knob Lock** - One locking control for both tuning knobs, more positive locking arrangement possible.
8. **Automatic Tuning** - The simpler design would be more easily adapted to future automatic tuning.

b. Disadvantages

1. **Increased Frequency Spacing** - Frequency spacing of 10 percent for 40-dB isolation between transceiver ports as compared to 5 percent for the present design. The alternate design would provide at least 28 dB of isolation between transceiver ports at 5-percent frequency spacing. Some tuning interaction may be present between channels at 5-percent spacing because of the reduced isolation.
2. **Increased Tuning Knob Rotation** - Slew function eliminated requiring more knob rotations to change frequency. Overall tuning time remains about the same since the additional knob rotation is offset by the fact that only 2 knobs require adjustment, and the phasing step has been eliminated.

4.3 SPECIFICATION CHANGES TO INCORPORATE ALTERNATE DESIGN

The following changes to Electronic Command Development Specification DS-AF-0169A(A), dated 21 June 1974, would be required to incorporate the alternate design.

Paragraph 3.3.4 should be changed to read as follows:

3.3.4 **Insertion Loss.** The insertion loss shall be as low as possible with the following maximum specification including effects of temperature.

3.3.4.1 **Two-Channel Configuration:** 1.40 dB

3.3.4.2 **Five-Channel Configuration:** 1.65 dB

3.3.4.3 **Ten-Channel Configuration:** 2.15 dB

Paragraph 3.3.5 should be changed to read:

3.3.5 Isolation. For frequency separations of 10 percent or more, the multicoupler shall provide at least 40-dB isolation between transceiver input terminals.

Paragraph 3.3.10 should be changed to read:

3.3.10 Size. An effort shall be made to produce a small size package, consistent with the other requirements of this specification. The maximum size shall be 125 cubic inches per filter module, excluding knobs, switches, and mounting flanges.

Section 5

Conclusion

This program has provided a firm basis for the development of a manually tuned multicoupler having up to 10 communication channels. The techniques developed for combining the bandpass filters into a multicoupler configuration are well defined. Operation at the specified rf power level (60 watts per channel) has been achieved by employing a newly developed gas filled variable tuning capacitor. IMD performance has been improved over equipment delivered on a prior contract. However, a specification change to reduce the IMD requirement on third order, intermod to 120 dB below 60 watts for signals separated by 5 percent or more is suggested.

Two other minor problems found during environmental testing can easily be corrected. No other specification changes are required except for IMD.

The basic design approach is sound. A bandpass filter design has been achieved that can be used singly or combined to form multicouplers without requiring any change to the basic filter. The matching network and combining techniques developed provide good performance, require no adjustment, and provide interaction free tuning of the bandpass filters.

The alternate design approach discussed in section 4 looks very attractive from the standpoint of reduced size, weight, cost, and insertion loss. It also offers greater simplicity in regard to tuning, requiring fewer controls and less adjustments. This is an important consideration in a manually tuned equipment. The transition from the present design to the alternate approach would involve essentially no risk since the same techniques would be applicable. The only disadvantage of the alternate design, of any consequence, is the reduced selectivity. If 10-percent channel spacing (40-dB isolation between channels) can be tolerated instead of the present 5-percent spacing, there is little doubt that the alternate design should be selected.

Section 6

Literature Cited

1. S. B. Cohn, "Dissipation Loss in Multiple-Coupled-Resonator Filters," Proceedings of the IRE, pp 1342-1348 (August 1959).
2. H. L. Landt, "Design of Minimum Loss Filters Using Any Number of Resonators," WP-4738, January 23, 1967, Collins Radio Company, Cedar Rapids, Iowa.
3. G. L. Matthaei, "Synthesis of Tchebycheff Impedance-Matching Networks, Filters, and Interstages," IRE Trans. PGCT 3, pp 162-172 (September 1956).
4. A. I. Zrerev, "Handbook of Filter Synthesis" Wiley, New York, 1967.
5. George L. Matthaei, Leo Young, E. M. T. Jones, "Microwave Filters, Impedance-Matching Networks, and Coupling Structures," McGraw-Hill, 1964, p 100.
6. R. M. Fano, "Theoretical Limitations on the Broadband Matching of Arbitrary Impedances," J. Franklin Inst, Vol 249, pp 57-83 and 139-154 (January and February 1950).

DISTRIBUTION LIST

101	Defense Documentation Center ATTN: DDC-TCA Cameron Station (Bldg 5) Alexandria, VA 22314	012	
104	Defense Communications Agency Technical Library Center Code 205 (P. A. Tolovi) Washington, DC 20305	001	
110	Code R121A, Tech Library DCA/Defense Comm Engring Ctr 1860 Wiehle Ave Reston, VA 22090	001	
200	Office of Naval Research Code 427 Arlington, VA 22217	001	
205	Director Naval Research Laboratory ATTN: Code 2627 Washington, DC 20375	001	
206	Commander Naval Electronics Laboratory Ctr ATTN: Library San Diego, CA 92152	001	
207	Commander US Naval Surface Weapons Ctr ATTN: Library Code WX-21 White Oak, Silver Sprg, MD 20910	001	
208	Commanding Officer NAVENVPREDRSCHFAC Tech Library Monterey, CA 93940	002	
210	Commandant, Marine Corps HQ, US Marine Corps ATTN: Code LMC Washington, DC 20380	001	
211	HQ, US Marine Corps ATTN: Code INIS Washington, DC 20380	001	
212	Command, Control & Comm Div Development Center Marine Corps Dev & Educ Cmd Quantico, VA 22134	001	
214	CDR, Naval Air Systems Command Meteorological Div (AIR-05F) Washington, DC 20361	001	
215	Naval Telecommunications Cmd Tech Library, Code 91L 4401 Massachusetts Ave. NW Washington, DC 20390	001	
301	Rome Air Development Center ATTN: Documents Library (TILD) Griffiss AFB, NY 13441	001	
303	AFGWC/DO Offutt AFB, NE 68113	001	
304	Air Force Geophysics Lab L. G. Hanscom Field ATTN: LIR Bedford, MA 01730	001	
307	HQ ESD (DRI) L. G. Hanscom Field Bedford, MA 01730	001	
313	Armament Development & Test Center ATTN: DLOSL, Tech Library Eglin Air Force Base, FL 32542	001	
314	HQ, Air Force Systems Command ATTN: DLCA Andrews AFB Washington, DC 20331	001	
401	Commander HQ, TRADOC ATTN: ATTNG-XO Ft. Monroe, VA 23651	001	
405	Deputy for Science & Technology Ofc Assist Sec Army (R&O) Washington, DC 20310	001	
406	Commander US Army Training & Doctrine Cmd ATTN: ATCD-TEC Fort Monroe, VA 23651	001	
407	Commander US Army Training & Doctrine Cmd ATTN: ATCD-SIE Fort Monroe, VA 23651	001	

409	Commander, DARCOM ATTN: DRCMA-EE 5001 Eisenhower Ave Alexandria, VA 22333	001	001	Commandant US Army Field Artillery School ATTN: ATSFA-CTD Fort Sill, OK 73503
414	Commander US Army Training & Doctrine Cmd ATTN: ATCD-TM Fort Monroe, VA 23651	001	435	Commandant US Army Air Defense School ATTN: ATSA-CD-MC Fort Bliss, TX 79916
416	Commander US Army R&D Group (Far East) APO, San Francisco 96343	004	436	Commandant US Army Engineer School ATTN: ATSE-TD-TL Fort Belvoir, VA 22060
419	Commander US Army Missile Command ATTN: DRSMI-RRA, Bldg 7770 Redstone Arsenal, AL 35809	001	442	Cdr, Harry Diamond Laboratories ATTN: Library 2800 Powder Mill Road Adelphi, MD 20783
421	CDR, US Army Missile Command Redstone Scientific Info Ctr ATTN: Chief, Document Section Redstone Arsenal, AL 35809	002	450	Commander Frankford Arsenal ATTN: Library, K2400, B1. 51-2 Philadelphia, PA 19137
422	Commander US Army Aeromedical Research Lab ATTN: Library Fort Rucker, AL 36362	001	455	Commander White Sands Missile Range ATTN: STEWS-ID-S HQ White Sands Missile Range, NM 88002
423	Commander US Army Armament Command ATTN: DR SAR-RDP (Library) Rock Island, IL 61201	001	458	Dir/Dev & Engr Defense Systems Div ATTN: SAREA-DE-DDR, H. Tannenbaum Edgewood Arsenal, APG, MD 21010
427	CDR, US Army Combined Arms Combat Developments Activity ATTN: ATCA-COE-I Fort Leavenworth, KS 66027	003	465	Commander Aberdeen Proving Ground ATTN: STEAP-TL (Bldg 305) Aberdeen Proving Ground, MD 21005
429	Commander US Army Logistics Center ATTN: ATCL-MA Fort Lee, VA 23801	001	475	Commander HQ, Fort Huachuca ATTN: Technical Reference Division Fort Huachuca, AZ 85613
430	Commandant US Army Ordnance School ATTN: ATSL-CD-OR Aberdeen Proving Grnd, MD 21005	001	476	Commander US Army Electronic Proving Ground ATTN: STEEP-MT Fort Huachuca, AZ 85613
431	Commander US Army Intelligence Center & School ATTN: ATSIT-CD-MD Fort Huachuca, AZ 85613	001	480	Commander USASA Test and Evaluation Center ATTN: IAO-CDR-T Fort Huachuca, AZ 85613

483	Cdr, US Army Research Office ATTN: DRXRO-IP PO Box 12211	525	Project Manager, REMBASS ATTN: DRCPM-RBS
001	Research Triangle Park, NC 27709	001	Fort Monmouth, NJ 07703
490	Commander Edgewood Arsenal ATTN: SAREA-TS-L	526	Project Manager, NAVCON ATTN: DRCPM-NC-TM Bldg 2539
001	Aberdeen Proving Grnd, MD 21010	001	Fort Monmouth, NJ 07703
493	Director US Army Engr Waterways Exp Sta ATTN: Research Center Library	596	Commandant US Army Signal School ATTN: ATSN-CTD-MS
002	Vicksburg, MS 39180	002	Fort Gordon, GA 30905
500	Commander US Army Yuma Proving Ground ATTN: STEYP-MTD (Tech Library)	598	Commander US Army Satellite Comm Agency ATTN: DRCPM-SC-3
002	Yuma, AZ 85364	001	Fort Monmouth, NJ 07703
502	CO, US Army Tropic Test Ctr ATTN: STETC-MO-A (Tech Library)	610	Director, Night Vision Laboratory US Army Electronics Command ATTN: DRSEL-NV-D
001	Fort Clayton, Canal Zone 09827	001	Fort Belvoir, VA 22060
505	CDR, US Army Security Agency ATTN: IARDA-IT Arlington Hall Station	613	Atmospheric Sciences Lab, ECOM ATTN: DRSEL-BL-SY-1
001	Arlington, VA 22212	001	White Sands Missile Range, NM 88602
509	Commander US Army Logistics Center ATTN: ATCL-MC	617	Chief Intel Materiel Dev & Support Ofc Electronic Warfare Lab, ECOM
001	Fort Lee, VA 22801	001	Fort Meade, MD 20755
512	Directorate of Combat Developments US Army Armor School ATTN: ATZK-CD-MS	680	Commander US Army Electronics Command
001	Fort Knox, KY 40121	000	Fort Monmouth, NJ 07703
514	Commandant US Army Inst for Mil Asst ATTN: ATSU-CTD-MO	1	DRSEL-PP-I-PI
001	Fort Bragg, NC 28307	1	DRSEL-PL-ST
517	Commander US Army Missile Command ATTN: DRSMI-RE (Mr. Pittman)	1	DRSEL-VL-D
001	Redstone Arsenal, AL 35809	1	DRSEL-WL-D
519	Commander US Army Systems Analysis Acty ATTN: DRXSY-T	1	DRSEL-TL-D
001	APG, MD 21005	3	DRSEL-CT-D
		1	DRSEL-BL-D
		3	DRSEL-NL-RN-3
		1	DRSEL-NL-D-8
		1	DRSEL-SI-CM
		1	DRSEL-MA-MP
		2	DRSEL-MS-TI
		1	DRSEL-GG-TD
		1	DRSEL-CG (Mr. Doxey)
		2	DRSEL-PA
		1	USMC-LNO
		1	DRSEL-GS-H
		1	DRSEL-RD
		1	TADOC-LNO
		25	Orig Ofc DRSEL-NL-RN-3

701 MIT - Lincoln Laboratory
ATTN: Library - Rm A-082
POB 73
001 Lexington, MA 02173

703 NASA Scientific & Tech Info Facility
ATTN: Acquisitions Branch (S-AK/DL)
PO Box 33
002 College Park, MD 20740

704 National Bureau of Standards
Bldg 225, Rm A-331
ATTN: Mr. Leedy
001 Washington, DC 20231

706 Advisory Group on Electron Devices
ATTN: Secy, Working Group D (Lasers)
201 Varick St
002 New York, NY 10014

708 Ballistic Missile Radiation Anal Cen
Env Research Inst of Michigan
Box 618
001 Ann Arbor, MI 48107

711 Metals and Ceramics Inf Center
Battelle
505 King Avenue
001 Columbus, OH 43201

713 R. C. Hansen, Inc.
PO Box 215
001 Tarzana, CA 91356

714 Ketron, Inc.
ATTN: Mr. Frererick Leuppert
1400 Wilson Blvd, Architect Bldg
001 Arlington, VA 22209

720 CINDAS
Purdue Industrial Rsch Park
2595 Yeager Rd
001 W. Lafayette, IN 47906